Anamet, inc Materials Engineering & Laboratory Testing
26102 EDEN LANDING ROAD, SUITE 3 • HAYWARD, CALIFORNIA 94545 • (510) 887-8811 • FAX (510) 887-8427

Report No. 5004.7920 C Rev. 2 **April 15, 2013**

METALLURGICAL EVALUATION OF PIPE SAMPLES FROM THE CHEVRON USA INC., EL SEGUNDO REFINERY #4 CRUDE UNIT 8-INCH DIAMETER 4-SIDECUT

Customer Authorization: Contract CSB-12-C-002

Report To: Chemical Safety and Hazard Investigation Board
Attn: Roger Evans
2175 K Street, NW, Suite 400
Washington, DC 20037

1.0 INTRODUCTION

Seven samples of 8-inch diameter 4-sidecut from the Chevron USA, Inc. (CUSA) El Segundo refinery #4 Crude Unit were submitted by CUSA and the Chemical Safety and Hazard Investigation Board (CSB) for metallurgical evaluation. It was reported that the sampled line had been constructed of Schedule 40 carbon steel in the 1970's and was removed from service as a precaution following the August 6, 2012 incident at the CUSA Richmond refinery sister unit. The purpose of this evaluation was to compare the condition of the El Segundo 8-inch 4-sidecut samples to those from the CUSA Richmond refinery described in Anamet, Inc. Report No. 5004-7920 B.

The samples were evaluated by the following laboratory procedures:

1) Visual and macroscopic examination
2) Chemical analysis
3) Tensile testing
4) Metallography
5) Energy dispersive X-ray spectroscopy
6) X-ray diffraction

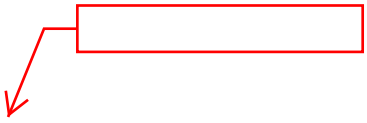

Based on the results of this evaluation, sulfidation corrosion had generally affected the CUSA El Segundo samples to a similar extent as the CUSA Richmond samples had been generally affected. In contrast with the Richmond samples, the thinnest measured pipe wall was 0.128-inch, found in sample ELS-1, which was removed from a location comparable to downstream from the rupture location in the Richmond 4-sidecut. The well recognized correlation between greater sulfidation corrosion rates and silicon concentrations below 0.10-wt% was also observed with these samples.

2.0 EVALUATION[1]

2.1 Visual Examination

Sample identifications are listed in Table 1 along with a short description. The locations from which the samples were removed from the 4-sidecut are shown in Appendix A. The location and 30° down slope of sample ELS-5 corresponded closely with the ruptured section of Richmond 8-inch 4-sidecut. The samples are shown in the as-received condition in Figure 1 through Figure 4.

Combinations of adherent scale and loose rust were present on the outside surfaces of all the samples, consistent with the service life and reported exposed outdoor storage of the samples after the removal from service. Various combinations of dark gray to black scale were present on the inside surfaces. Near flame cut ends, this scale was mostly absent. In some samples, a rust red tint was present, an indication of rust formation during storage. The appearance of the inside scale was similar to that observed in the Richmond samples.

No evidence of pipe deformation or rupture was present, with the exception of a small dent on the outside surface of sample ELS-2. Disturbance of the scale indicated that the dent occurred recently, likely during removal of the line from service. An apparent difference in wall thickness was observed between pipe spools in sample ELS-4 and ELS-5. Metallography, described in Section 2.4, demonstrated a difference in wall thickness attributable to sulfidation corrosion in these two locations.

Wall thickness measurements were made with dial calipers after removing loose scale from the inside and outside surfaces at the section locations indicated in Figure 1 through Figure 4. The samples were not clearly marked with respect to vertical orientation, so in most cases the measurements were made at arbitrary locations spaced 90° around the pipe circumference. Measured wall thickness values are listed in Table 2. The thinnest pipe wall listed in Table 2 is 0.134-inch, found in specimen ELS-1. This sample was in a location comparable to downstream from the ruptured section of 4-sidecut in the Richmond refinery. The nominal wall thickness of 8-inch Schedule 40 pipe is 0.322-inch.

The average of all wall thickness values listed in Table 2 is 0.196-in. Wall thickness values from the Richmond 8-inch 4-sidecut samples are listed in Table 3, reproduced here from Anamet report 5004.7920 B.[2] To compare the general extent to which sulfidation corrosion had affected the El Segundo 8-inch 4-sidecut and the Richmond 8-inch 4-sidecut, the average value of thickness values in Table 3 was calculated. The thickness values in the shaded rows of Table 3 were discarded to avoid over sampling of the ruptured section, to include only pipe thickness values, and to represent the same number of thickness readings as were used for the El Segundo average thickness calculation. The resulting average thickness for the Richmond samples was 0.220-inch. The similarity of the average thickness values is not surprising given the similarity

[1] The magnifications of the optical and scanning electron micrographs in this report are approximate and should not be used as a basis for dimensional analyses unless otherwise indicated.

[2] Anamet Report No. 5004.7920 B, FINAL REPORT**:** METALLURGICAL EVALUATION OF SAMPLES FROM THE CHEVRON U.S.A. INC., RICHMOND #4 CRUDE UNIT 8-INCH AND 12-INCH 4-SIDECUT PIPING INVOLVED IN THE AUGUST 6, 2012, HYDROCARBON RELEASE AND FIRE, Prepared for The Chemical Safety and Hazard Investigation Board (CSB), February 5, 2013.

of the materials of construction, similarity of the service conditions, and similarity of the time in service between the El Segundo and Richmond 8-inch 4-sidecut piping.

Uneven or wavy wall loss, similar to that observed in the Richmond 4-sidecut samples, was investigated by cleaning specimens from the El Segundo 8-inch 4-sidecut by immersion in a 25% solution of Oakite® 33 and water. Alternating cycles of immersion in the solution and wire brushing the inside and outside surface scale removed the majority of the scales present. Photographs of the inside surfaces after cleaning are shown in Figure 5 through Figure 7. Uneven or wavy wall loss was present on all specimens examined except ELS-4-2, ELS-6 and ELS-7. Thickness measurements indicated in the figures were performed using a pointed anvil micrometer at locations selected to demonstrate the range of thickness associated with uneven wall loss on the cleaned specimens. The thinnest wall thickness measured was 0.128-inch on the cleaned specimen from ELS-1.

2.2 Chemical Analysis

Quantitative chemical analysis by optical emission spectroscopy (OES) and LECO combustion was performed on specimens sectioned from the samples. Analysis by OES was performed on the outside surface of the specimens after grinding down to bright metal. The locations from which specimens were sectioned are indicated in Figure 1 through Figure 4. Specimens were sectioned from two spools of pipe in each of samples ELS-4 and ELS-5, as indicated in Figure 2b and Figure 3a, respectively. The results are listed in Table 4 through Table 6. The chemical composition requirements for ASTM A 106 and ASTM A 53 Grade B carbon steel pipe are listed in Table 7. The important difference between these two standards with respect to sulfidation corrosion is ASTM A 106 specifies the acceptable range of silicon concentration, while ASTM A 53 does not.

2.3 Tensile Testing

Tensile specimens were machined from samples ELS-1, ELS-3, ELS-5, and ELS-6, sectioned from the locations indicated in Figure 1 through Figure 3. Testing was performed in accordance with ASTM E 370. Specimen gage length and width were 2.00-inches and 0.50-inches, respectively. Specimen gage thickness was determined by the steel remaining after machining the outside surface flat and removal of all visible evidence of gray scale from the inside surface. Results are listed in Table 8. The tensile and yield strength requirements for ASTM A 106 and ASTM A 53, Grade B, pipe are listed in Table 9. The tested specimens met the stated requirements.

2.4 Metallography

Metallography was performed on longitudinal specimens prepared from each sample. The locations of the sections in each sample are indicated in Figure 1 through Figure 4, and representative micrographs of the interface between the inside surface and the inside scale are shown in Figure 8 through Figure 14. In each specimen, the light gray scale was consistent with iron sulfide formed by sulfidation corrosion of carbon steel.

Photographs of the specimens prepared through circumferential welds in samples ELS-4 and ELS-5 are shown in Figure 10. More extensive thinning of ELS-4-2 compared to ELS-4-1, and ELS-5-1 compared to ELS-5-2, correlates with the silicon concentrations of each of the pipe spools listed in Table 5. In Figure 10b, the outside surface of ELS-5-1 was offset from the outside surface of ELS-5-2 by 0.068-inch. To investigate the cause of the offset, additional sections were cut at 90° increments from the section shown in Figure 10b. Photographs of the sections are shown in Figure 11. The outside surfaces of ELS-5-1 and ELS-5-2 were nominally coplanar in the additional sections, which indicates the outside diameter of ELS-5-1 was around 0.070-inch larger than the spool ELS-5-2, and the two spools were not exactly coaxial.

2.5 Energy Dispersive X-ray Spectroscopy

Specimens of scale scraped from the inside surface of each sample were analyzed by energy dispersive X-ray spectroscopy[3] (EDS). Semi-quantitative analysis was performed on the oxygen (O), sulfur (S), and iron (Fe) peaks, ignoring the low intensity peaks for various other elements. The results, shown in Figure 15 through Figure 17, were consistent with the elemental composition of iron sulfide scale formed by sulfidation corrosion of carbon steel.

2.6 X-Ray Diffraction

Scale specimens were scraped from the inside surface of samples ELS-4 and ELS-5 using a stainless steel spatula. The outer layers of the scale were generally friable and easily removed. The scale closest to the steel surface was adherent, and scraping revealed a dark gray metallic luster. Some rust was visible within the scale specimens, which were washed with toluene to remove residual hydrocarbons and allowed to dry. Phase analysis by X-ray diffraction (XRD) was subcontracted to Evans Analytical Group (EAG) in Sunnyvale, CA, and the results are shown in Appendix B. The results indicated iron sulfide was the majority species in each of the two specimens.

3.0 DISCUSSION

Sulfidation corrosion, also called sulfidic corrosion, is caused by the chemical reaction between iron and sulfur to form iron sulfide, generally at temperatures above 450°F. In crude oil distillation, naturally occurring sulfur and sulfur compounds are available to react with steel components, particularly plain carbon steels. The service conditions of the El Segundo #4 Crude Unit 4-sidecut piping were similar to the service conditions of the Richmond #4 Crude Unit 4-sidecut piping, temperatures and pressures of about 640°F 58-psig, and in both cases the material of construction was Schedule 40 carbon steel. Consequently, it is not surprising that the presence of thick sulfide scale on the inside surfaces of the pipe, and generally uniform wall thinning indicate that sulfidation corrosion was active during service of the El Segundo 4-

[3] The EDS analysis method used here detects the presence of elements from boron (B) to uranium (U), atomic numbers from 5 to 92 in the periodic table. EDS data alone are, however, insufficient to differentiate chemical compounds such as oxides, hydroxides, or carbonates or to characterize organic materials that consist of carbon (C), hydrogen (H), and nitrogen (N) only.

sidecut, and that the general extent of sulfidation corrosion was similar in both systems. The obvious difference between the two 4-sidecut lines was that Richmond suffered more extensive corrosion in one component that resulted in rupture.

Variables that affect sulfidation corrosion rates in crude oil distillation are the total sulfur content of the oil, the sulfur species present in the oil, temperature of the system, flow conditions, and the composition of the steel. Industry experience has shown that sulfidation corrosion rates in carbon steel are known to increase with a decrease in silicon concentration below 0.10-wt%, and are relatively constant at silicon concentrations above 0.10-wt%, given all other variables remain the same. A general trend of increased wall loss with a decrease in silicon concentration was observed for the El Segundo 8-inch 4-sidecut samples. Although sulfidation corrosion rates of carbon steel can be low, over decades of service a difference in corrosion rate caused by variations in silicon concentration can lead to failure in low silicon components while higher silicon bearing components retain useful life. Furthermore, if low silicon components happen to be located where other variables, such as flow or concentration of sulfur species, increase the corrosion rate, the combined affects can lead to much greater than expected wall loss.

4.0 CONCLUSIONS[4]

The following conclusions are based upon the submitted sample(s) and the evidence gathered:

1. Sulfidation corrosion had affected the CUSA El Segundo samples to a similar extent as the CUSA Richmond samples had been affected.

2. The thinnest pipe wall was 0.128-inch, measured in sample ELS-1 in a location comparable to downstream of where the Richmond 4-sidecut ruptured.

3. The well recognized correlation between greater sulfidation corrosion rates and silicon concentrations below 0.10-wt% was observed with these samples.

Prepared by:

Sam McFadden, Ph.D.
Associate Director of Laboratories

Reviewed by:

Ken Pytlewski, PE
Director, Engineering and Laboratories

[4] The conclusions in this report are based upon the available information and evidence provided by the client and gathered by Anamet, within the scope of work authorized by the client, and they are hereby presented by Anamet to a reasonable degree of engineering and scientific certainty. Anamet reserves the right to amend or supplement its conclusions or opinions presented in this report should additional data or information become available, or further work be approved by the client.

Table 1
List of 4-Sidecut Samples Examined

Identification	Description
ELS-1	One 12-inch long section of pipe, saw cut ends
ELS-2	Two 10-inch long sections of pipe joined by a 30° elbow, saw cut ends
ELS-3	One 20-inch long section of pipe joined to a 90° elbow, flame cut ends
ELS-4	Two 8-inch long sections of pipe joined to one leg of a tee, saw cut end on the pipe, flame cut ends on the tee
ELS-5	One 36-inch long section of pipe with welded pipe guides removed, joined to a 6-inch long section of pipe, flame cut ends
ELS-6	One 12-inch long section of pipe joined to one end of a 90° elbow, and 4-inches of pipe joined to the other end, saw cut ends
ELS-7	One 90° elbow joined to a tee, with a 2-inch long ring between the elbow and tee, flame cut ends

Table 2
Wall Thickness[A]

Sample	(in)	(in)	(in)	(in)
ELS-1	0.154	0.146	0.153	0.151
ELS-2	0.160	0.148	0.160	0.153
ELS-3	0.160	0.147	0.134	0.166
ELS-4-2	0.246	0.229	0.215	0.220
ELS-5-1	0.155	0.190	0.174	0.145
ELS-6	0.270	0.260	0.265	0.280
ELS-7	0.251	0.218	0.280	0.250

[A] Measurements spaced approximately 90° apart, taken with calipers after cleaning inside and outside surfaces with a wire brush.
[B] The nominal wall thickness of 8-inch diameter Schedule 40 pipe is 0.322-inch.

Table 3
Richmond 8-inch 4-Sidecut Samples Measured Wall Thickness [A]

Sample	0° (in)	90° (in)	180° (in)	270° (in)
E-017[B]	-.-	0.178	0.255	0.285
E-017[C]	0.110	0.090	0.105	0.092
E-022B	0.236	0.184	0.245	0.229
E-023A[D]	0.082	0.088	0.113	0.068
E-023A[E]	0.242	0.245	0.255	0.245
E-023B	0.240	0.258	0.225	0.240
E-028B	0.192	0.205	0.196	0.208
E-030B	0.218	0.172	0.278	0.236
E-034B	0.306	0.319	0.279	0.320

[A] Measurements taken with calipers after cleaning inside and outside surfaces with a wire brush.
[B] Measurements taken on the upstream elbow, middle of bend
[C] Measurements taken on the downstream end of the ruptured section
[D] Measurements taken on the end of the ruptured section joined to the 30° elbow
[E] Measurements taken on the downstream end

Table 4
Quantitative Chemical Analysis Results for

Element		ELS-1 (wt%)	ELS-2 (wt%)	ELS-3 (wt%)
Carbon[A]	(C)	0.24	0.23	0.23
Chromium	(Cr)	0.01	0.01	0.01
Copper	(Cu)	0.02	0.02	0.02
Iron	(Fe)	Primary Constituent		
Manganese	(Mn)	0.71	0.71	0.72
Molybdenum	(Mo)	<0.01	<0.01	<0.01
Nickel	(Ni)	0.01	0.01	0.01
Phosphorus	(P)	0.006	0.005	0.005
Silicon	(Si)	0.01	0.01	0.01
Sulfur	(S)	0.024	0.022	0.023
Vanadium	(V)	<0.005	<0.005	<0.005

[A]Determined by LECO combustion, all others determined by OES

Table 5
Quantitative Chemical Analysis Results for

Element		ELS-4-1 [B] (wt%)	ELS-4-2 [B] (wt%)	ELS-5-1 [B] (wt%)	ELS-5-2 [B] (wt%)
Carbon[A]	(C)	0.19	0.25	0.26	0.18
Chromium	(Cr)	0.04	0.06	0.02	0.04
Copper	(Cu)	0.01	0.05	0.03	0.01
Iron	(Fe)	Primary Constituent			
Manganese	(Mn)	1.09	0.96	0.77	1.10
Molybdenum	(Mo)	0.01	0.02	0.01	0.01
Nickel	(Ni)	0.01	0.04	0.02	0.01
Phosphorus	(P)	0.010	0.008	0.021	0.010
Silicon	(Si)	0.27	0.07	0.03	0.27
Sulfur	(S)	<0.005	0.028	0.023	0.005
Vanadium	(V)	<0.005	<0.005	<0.005	<0.005

[A]Determined by LECO combustion, all others determined by OES
[B]Two specimens were analyzed from two different pipe spools in each of ELS-4 and ELS-5

Table 6
Quantitative Chemical Analysis Results for

Element		ELS-6 (wt%)	ELS-7 (wt%)
Carbon[A]	(C)	0.25	0.22
Chromium	(Cr)	0.06	0.02
Copper	(Cu)	0.05	0.01
Iron	(Fe)	Primary Constituent	
Manganese	(Mn)	0.96	0.58
Molybdenum	(Mo)	0.02	.01
Nickel	(Ni)	0.04	0.02
Phosphorus	(P)	0.009	0.014
Silicon	(Si)	0.07	0.17
Sulfur	(S)	0.031	0.010
Vanadium	(V)	<0.005	<0.005

[A]Determined by LECO combustion, all others determined by OES

Table 7
Chemical Composition Requirements
for ASTM A 106 and A 53 Grade B Carbon Steel Pipe

Element		Requirements for A 106 Grade B Carbon Steel (wt%)		Requirements for A 53 Type S Grade B Carbon Steel (wt%)	
		min	max	min	max
Carbon	(C)	-.-	0.30	-.-	0.30
Chromium[A]	(Cr)	-.-	0.40	-.-	0.40
Copper[A]	(Cu)	-.-	0.40	-.-	0.40
Iron	(Fe)	Primary Constituent		Primary Constituent	
Manganese	(Mn)	0.29	1.06	-.-	1.20
Molybdenum[A]	(Mo)	-.-	0.15	-.-	0.15
Nickel[A]	(Ni)	-.-	0.40	-.-	0.40
Phosphorus	(P)	-.-	0.035	-.-	0.05
Silicon	(Si)	0.10	-.-	Not Controlled	
Sulfur	(S)	-.-	0.035	-.-	0.045
Vanadium[A]	(V)	-.-	0.08	-.-	0.08

[A] For A 53 Type S Grade B, the total composition for these five elements shall not exceed 1.00 wt%

Table 8
Tensile Test Results

Sample	Specimen Gage Thickness (in)	Tensile Strength (ksi)	Yield Strength (ksi)	Elongation in 2.0-inch Gage Length (%)
ELS-1	0.098	68.40	45.60	19.5
ELS-3	0.117	65.30	43.60	17
ELS-5	0.110	71.20	44.10	21
ELS-6	0.227	75.00	49.10	28.5

Table 9
Minimum Tensile and Yield Strength Requirements

	Tensile Strength (ksi)	Yield Strength (ksi)
A 106 Grade B	60.00	35.00
A 53 Grade B	60.00	35.00

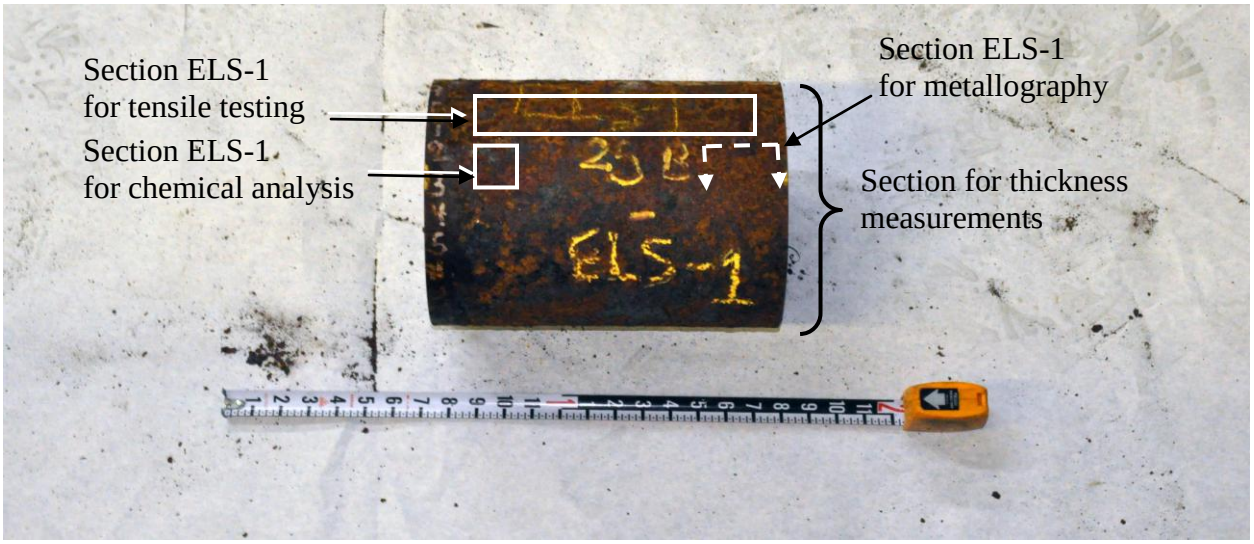

(a) ELS-1

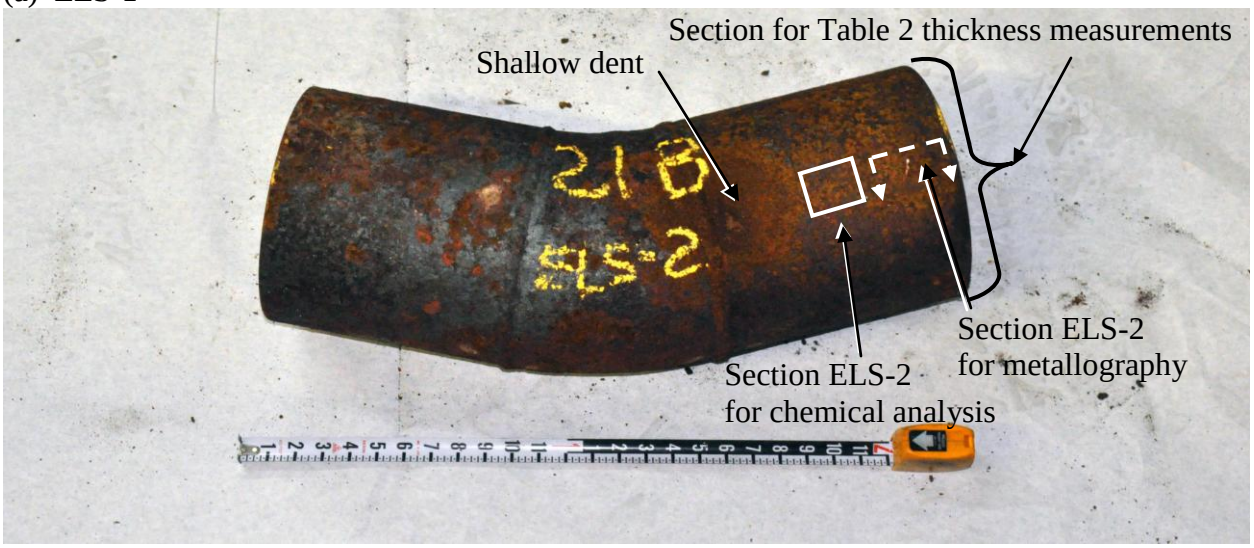

(b) ELS-2

Figure 1 Photographs of samples ELS-1 and ELS-2 as-received.

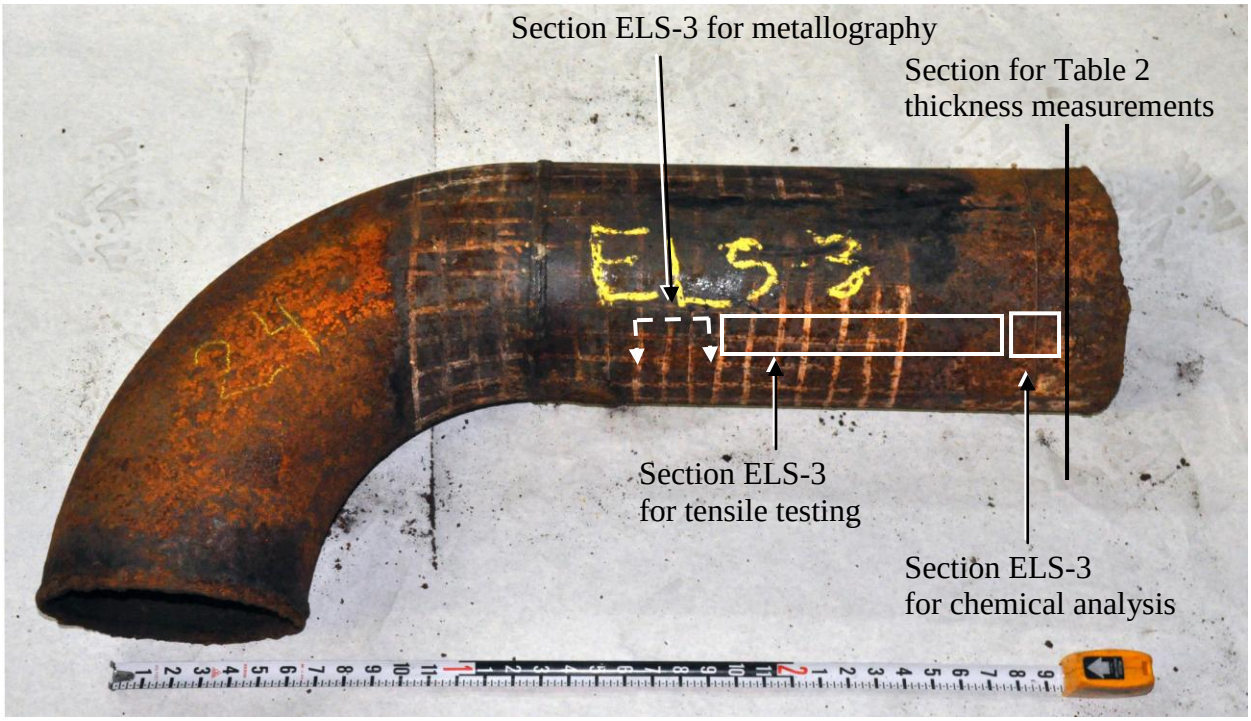

(a) ELS-3

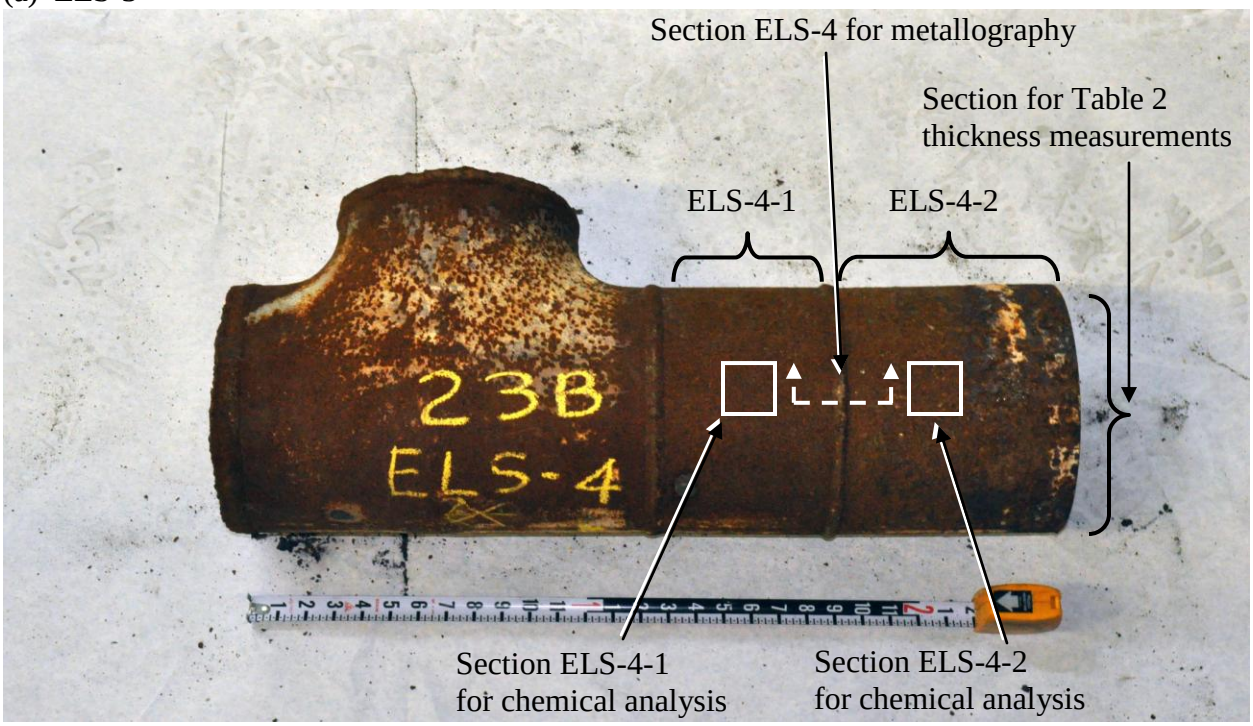

(b) ELS-4

Figure 2 Photographs of samples ELS-3 and ELS-4 as-received.

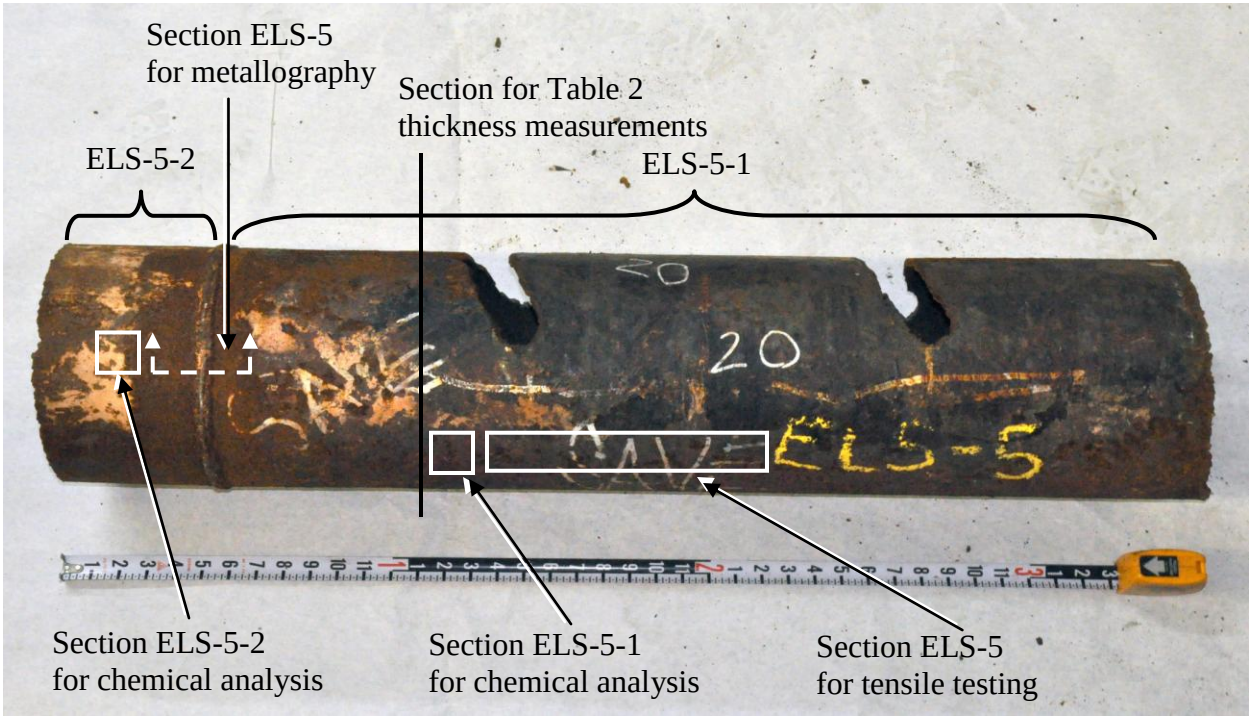

(a) ELS-5

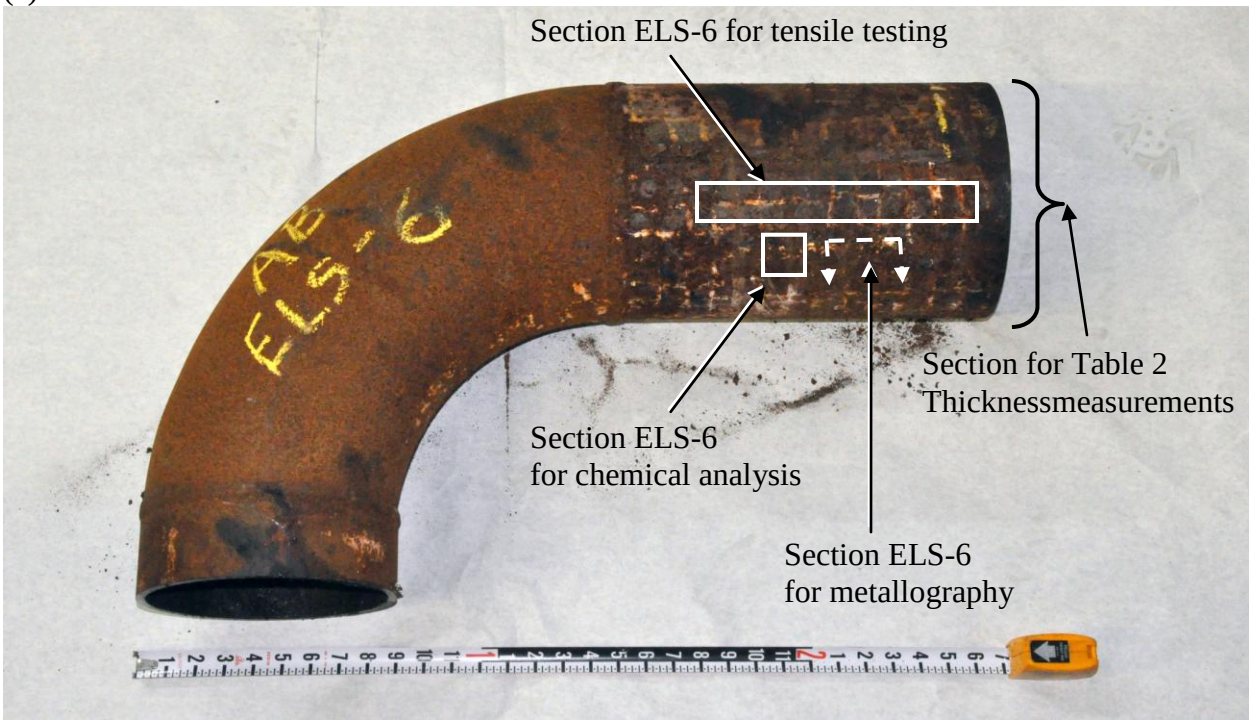

(b) ELS-6

Figure 3 Photographs of samples ELS-5 and ELS-6 as-received.

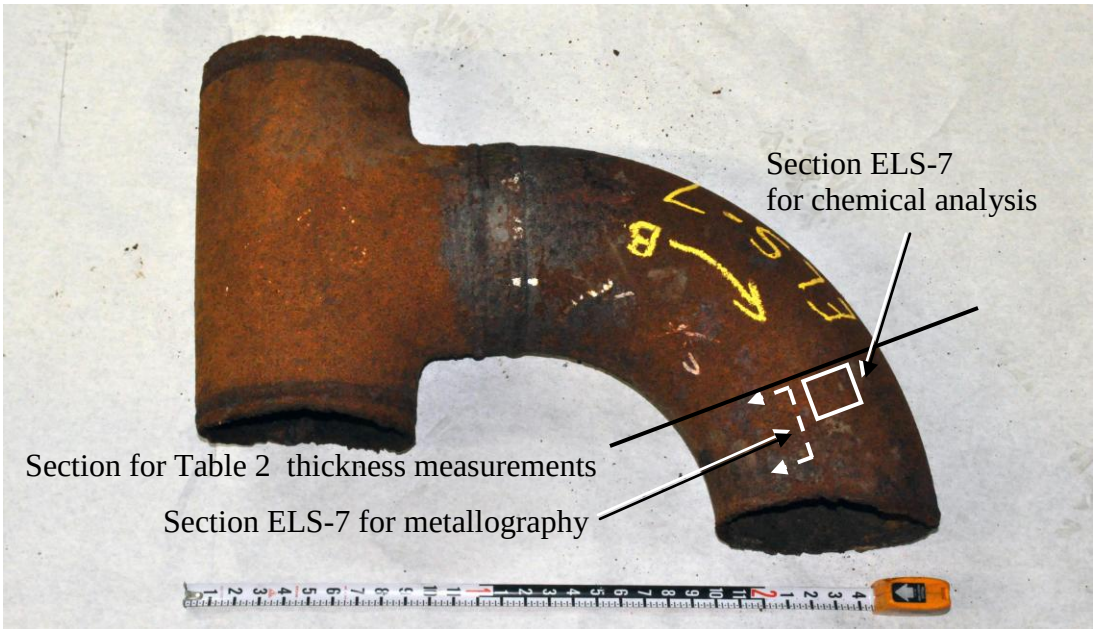

(a) ELS-7

Figure 4 Photograph of sample ELS-7 as-received.

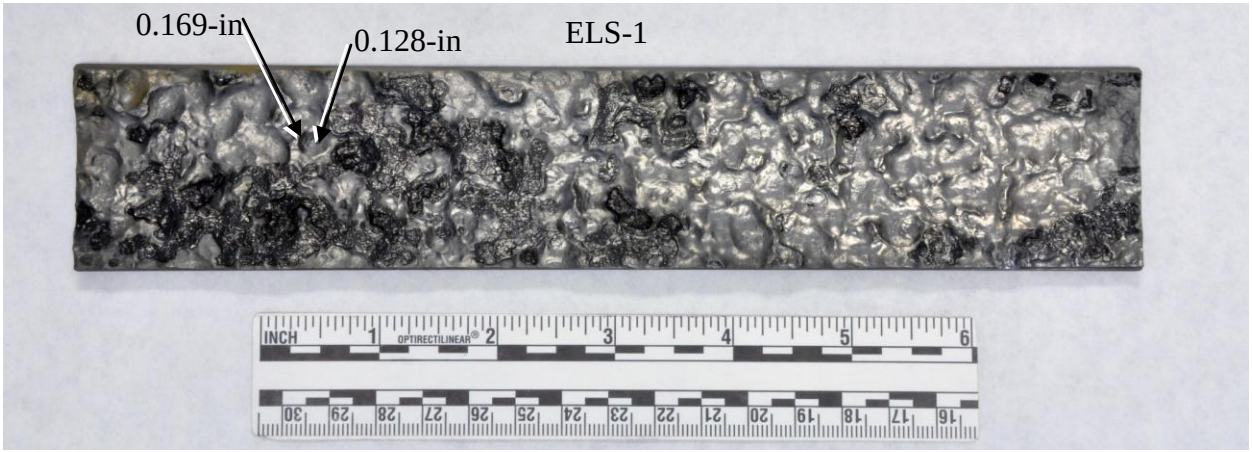

(a)

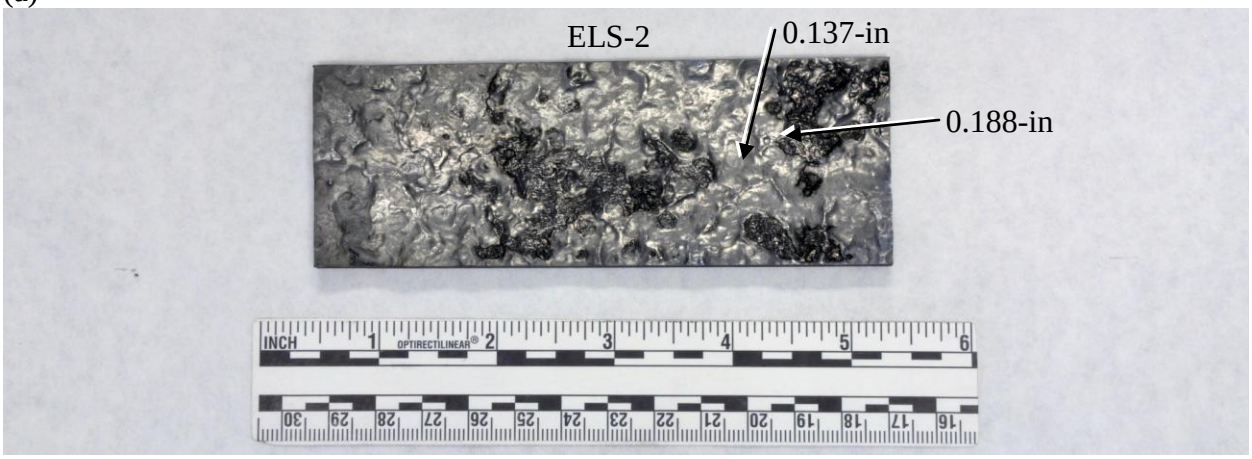

(b)

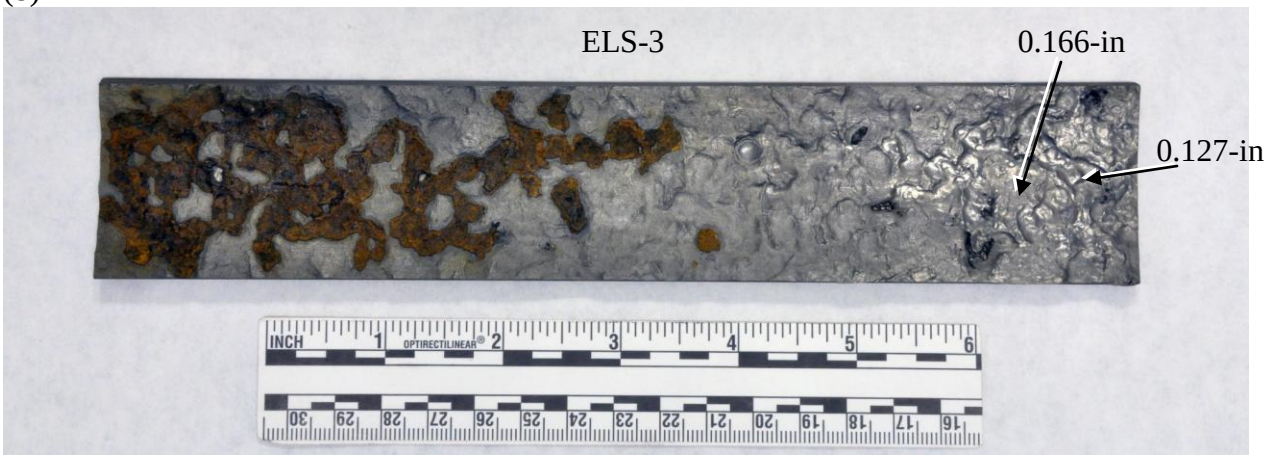

(c)

Figure 5 Photographs of the inside surfaces of specimens from samples ELS-1, ELS-2, and ELS-3 after cleaning. The specimens were sectioned from locations next to the specimens for chemical analysis.

(a)

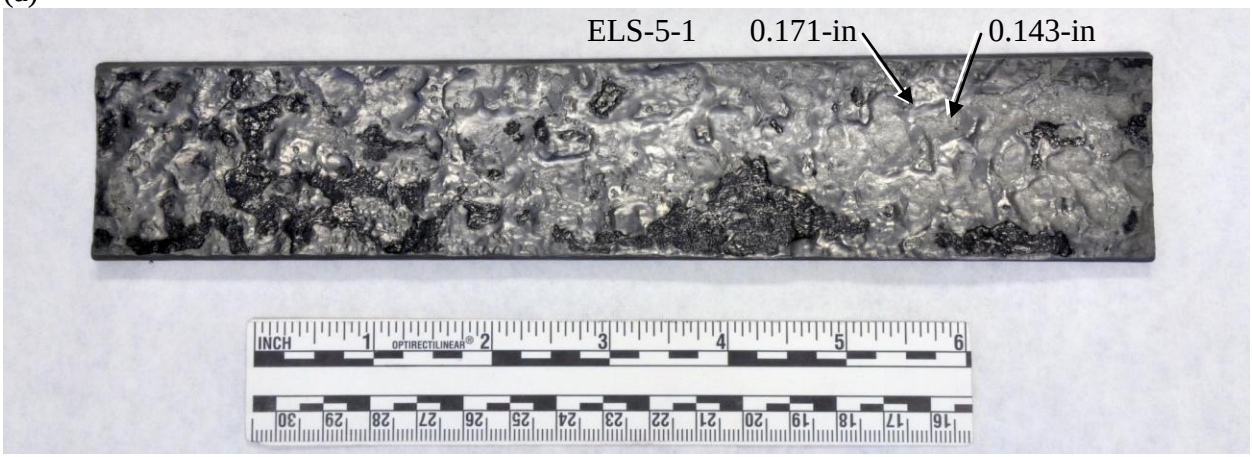

(b)

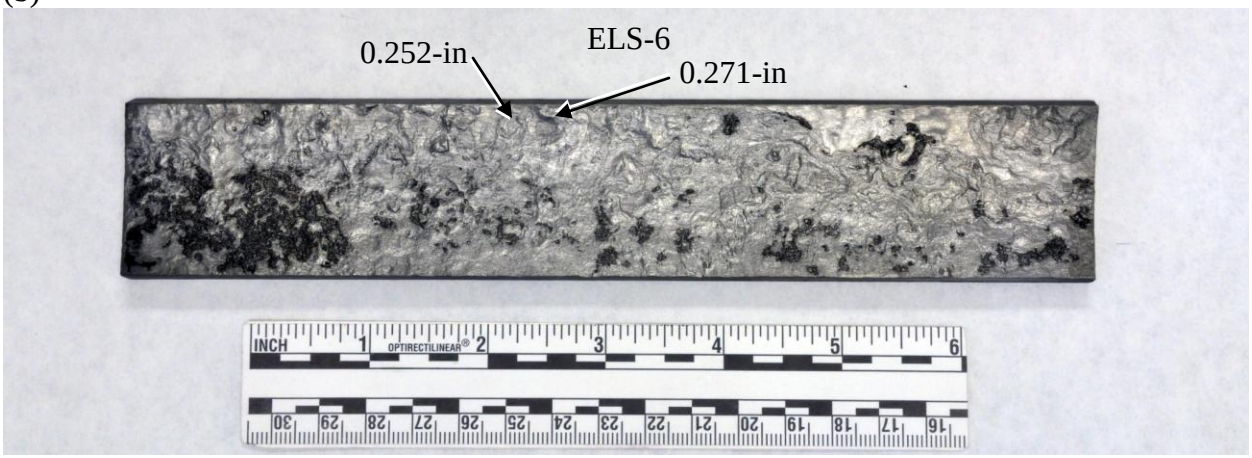

(c)

Figure 6 Photographs of the inside surfaces of specimens from samples ELS-4, ELS-5, and ELS-6 after cleaning. The specimens were sectioned from locations next to the specimens for chemical analysis.

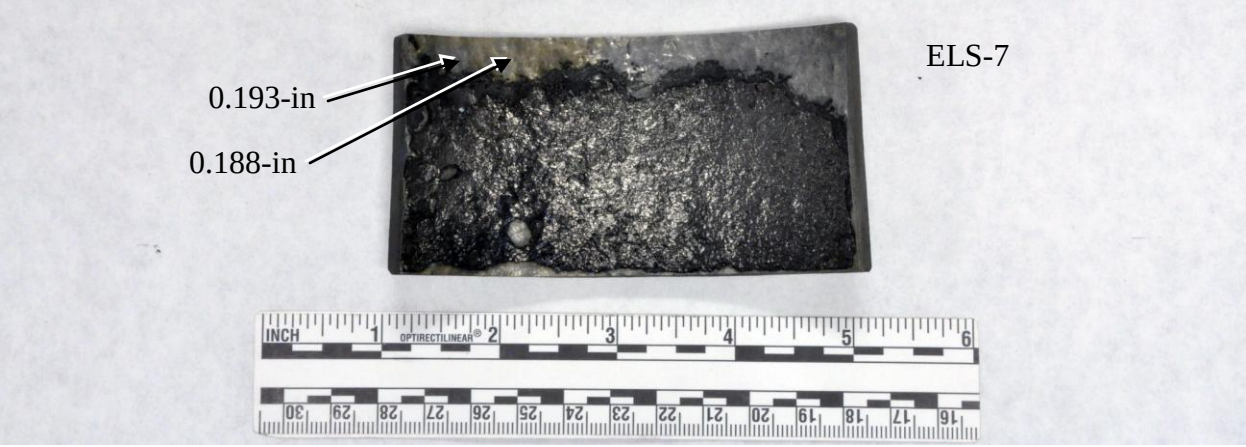

Figure 7 Photograph of the inside surface of a specimen from sample ELS-7 after cleaning. The specimen was sectioned from a location next to the specimen for chemical analysis.

(a) ELS-1 100X

Figure 8 Optical micrograph of a specimen prepared from sample ELS-1. The section location is indicated in Figure 1a.

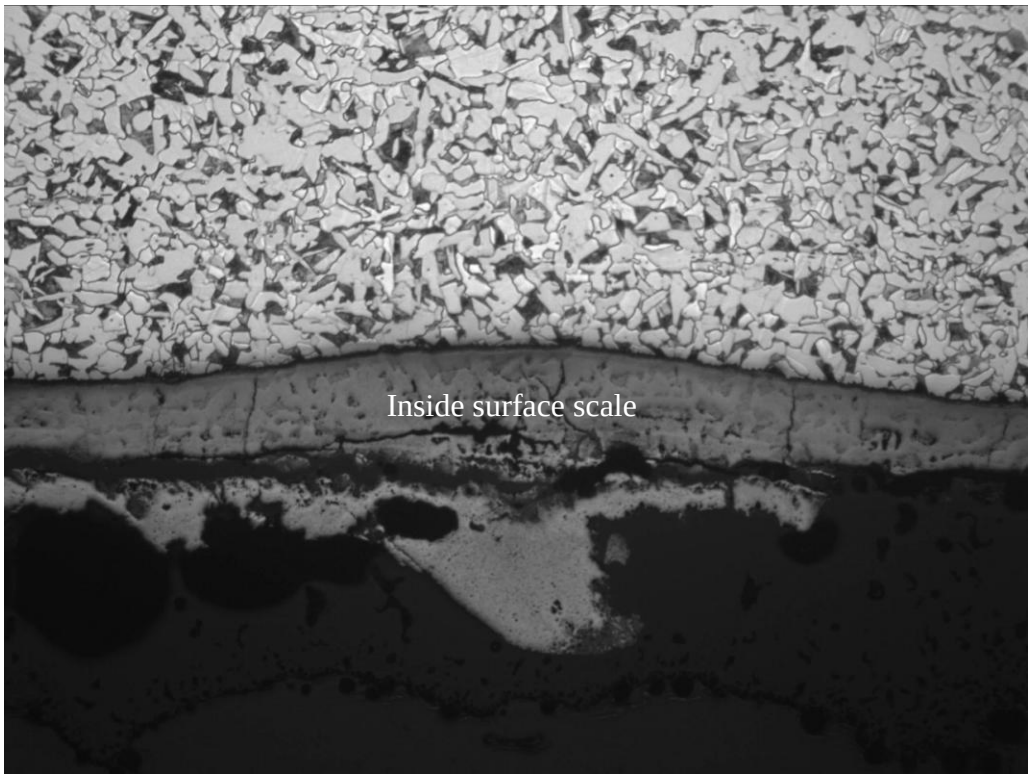

(a) ELS-2 100X

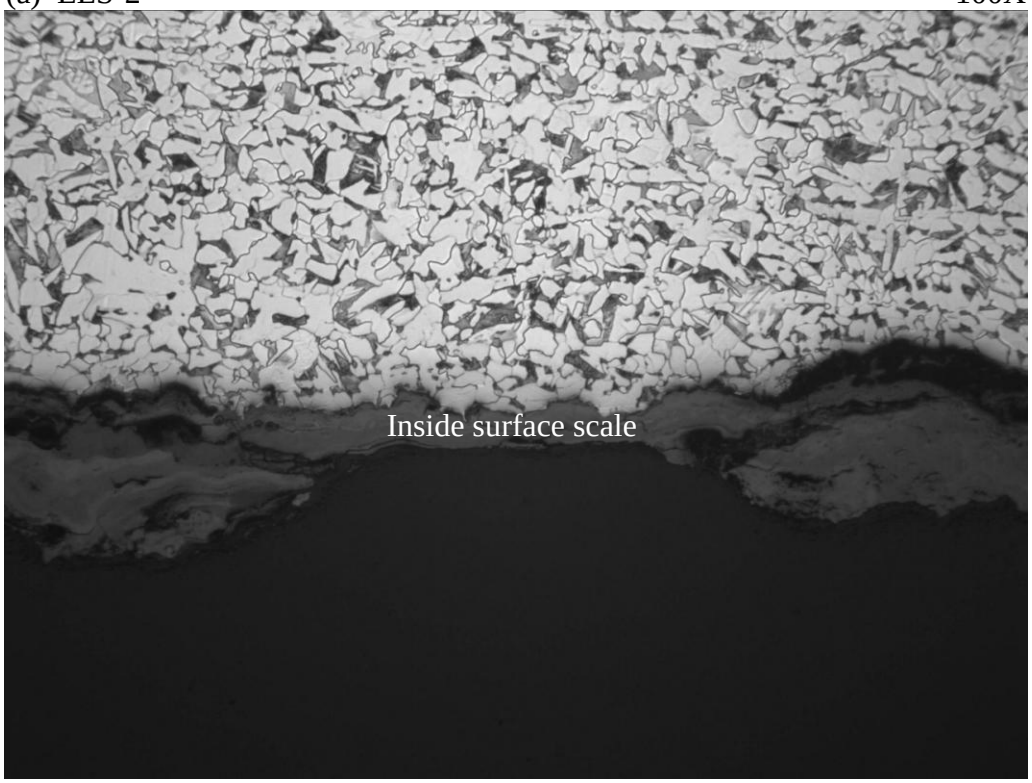

(b) ELS-3 100X

Figure 9 Optical micrographs of specimens prepared from samples ELS-2 and ELS-3. The section locations are indicated in Figure 1b and Figure 2a, respectively.

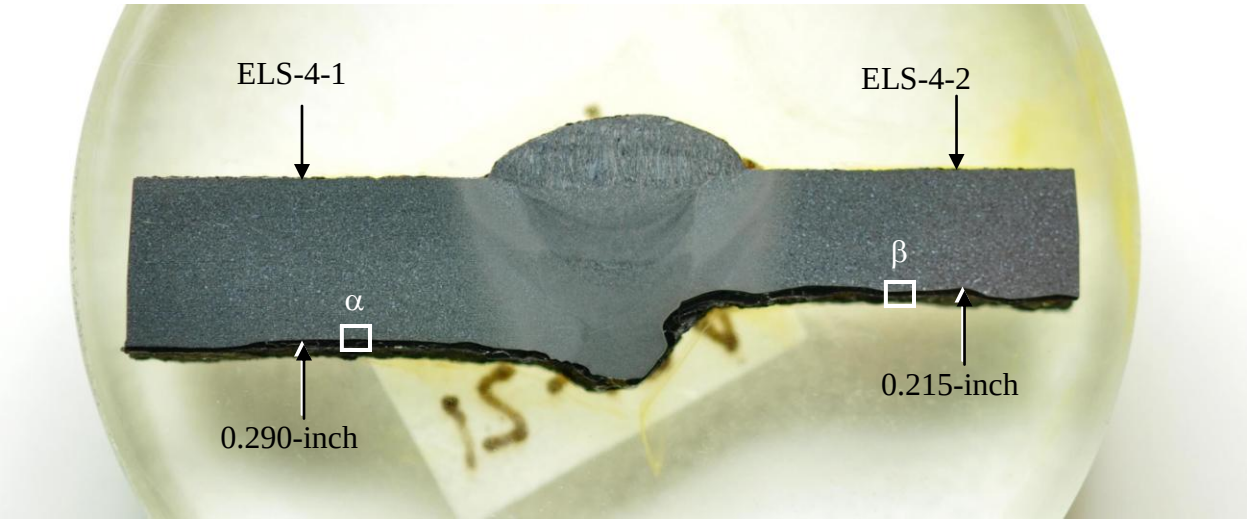

(a) ELS-4

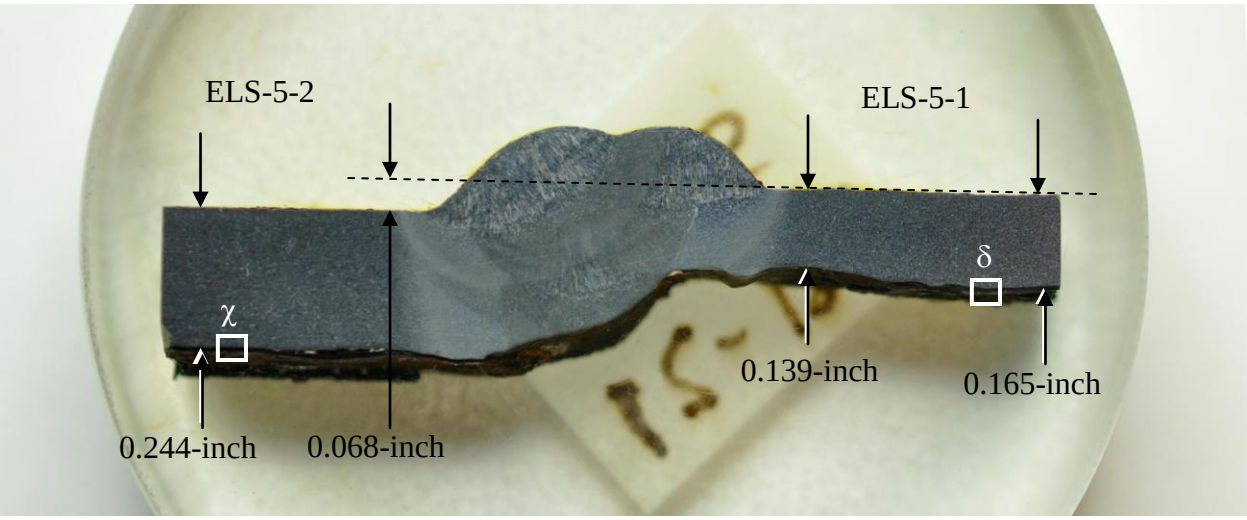

(b) ELS-5

Figure 10 Photographs of specimens prepared for metallography from the locations on samples ELS-4 and ELS-5 indicated in Figure 2b and Figure 3a, respectively. Optical micrographs of the boxed areas are shown in Figure 12 and Figure 13. The dashed line indicates the outside surface of ELS-5-1 was offset 0.068-inch from the outside surface of ELS-5-2.

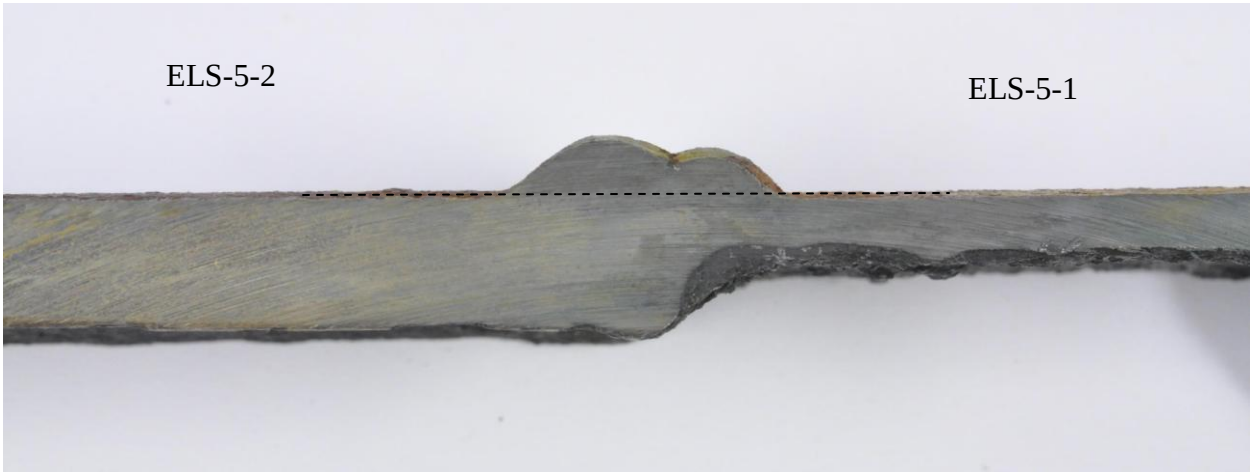

(a) 90°

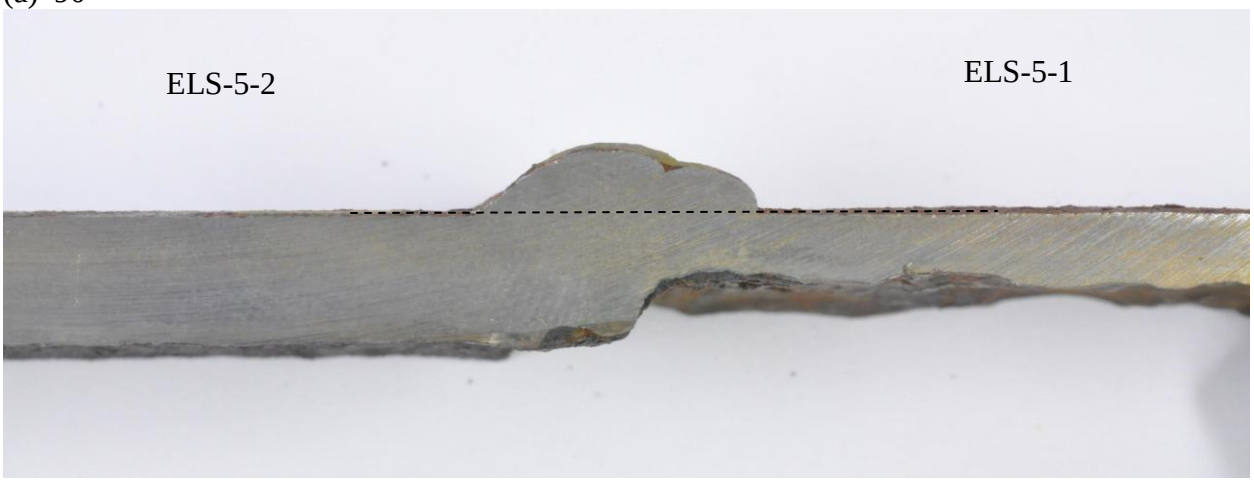

(b) 180°

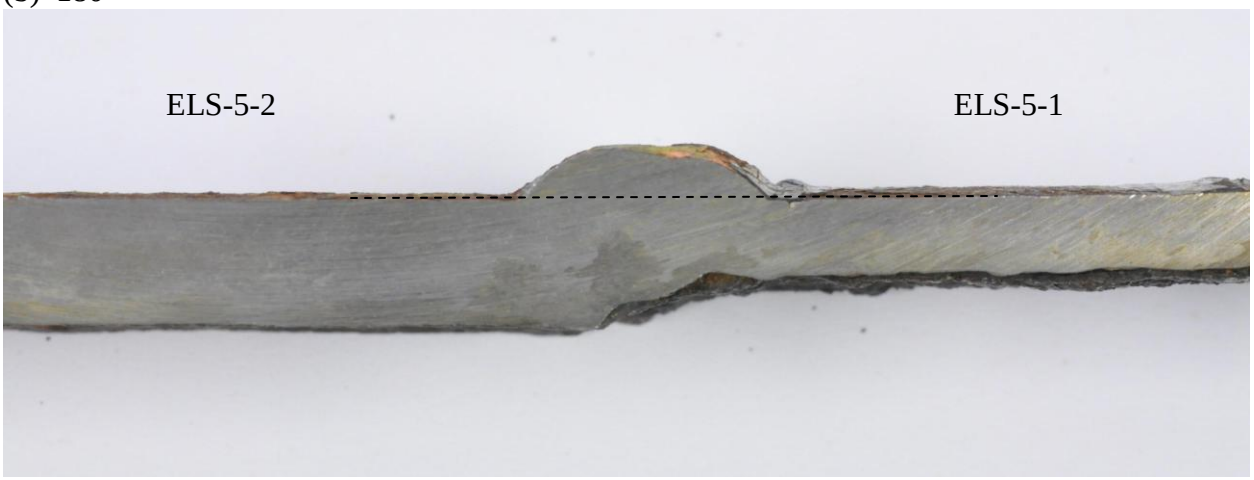

(c) 270°

Figure 11 Sections through sample ELS-5 taken 90°, 180°, and 270° from the section shown in Figure 10b. The outside surfaces of the two pipe spools were coplanar in these sections, as indicated by the dashed lines.

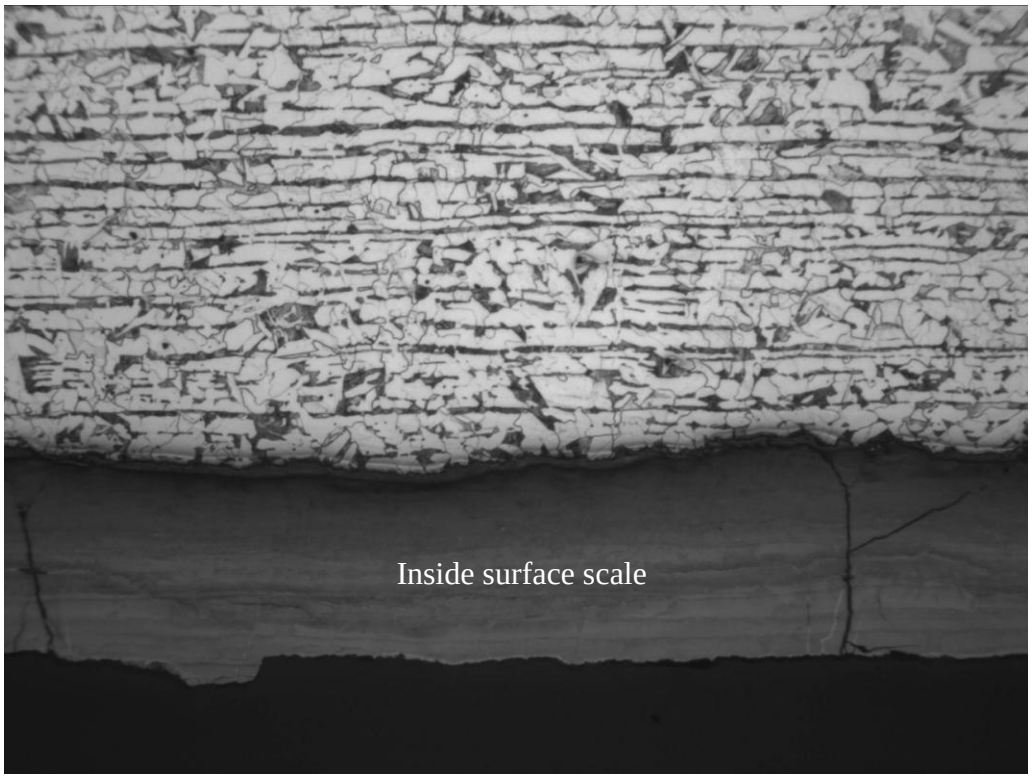

(a) ELS-4-1, area labeled α in Figure 10a 100X

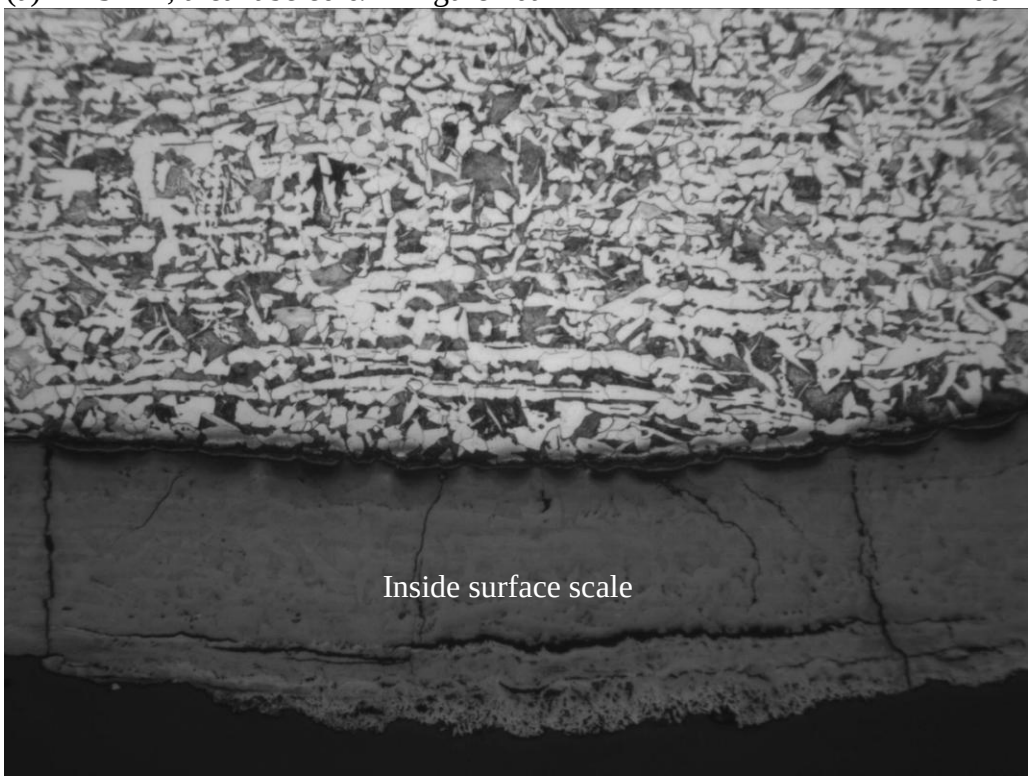

(b) ELS-4-2, area β in Figure 10a 100X

Figure 12 Optical micrographs of the specimen prepared from sample ELS-4 shown in Figure 10a. The section location is indicated in Figure 2b.

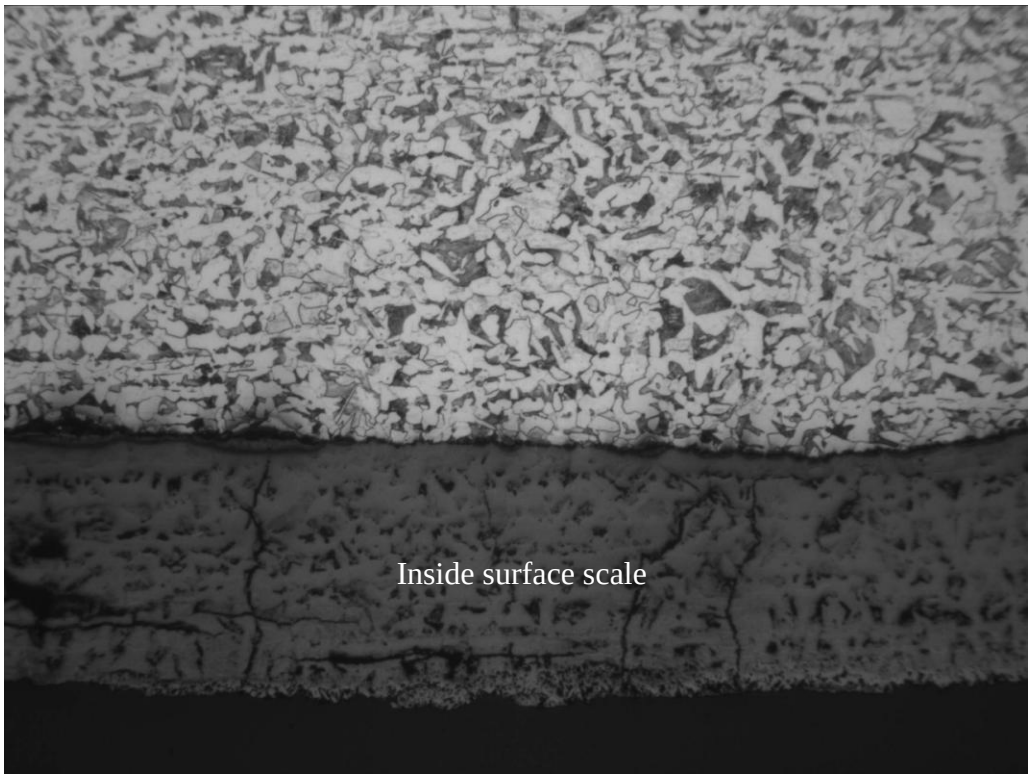

(a) ELS-5-1, area labeled δ in Figure 10b 100X

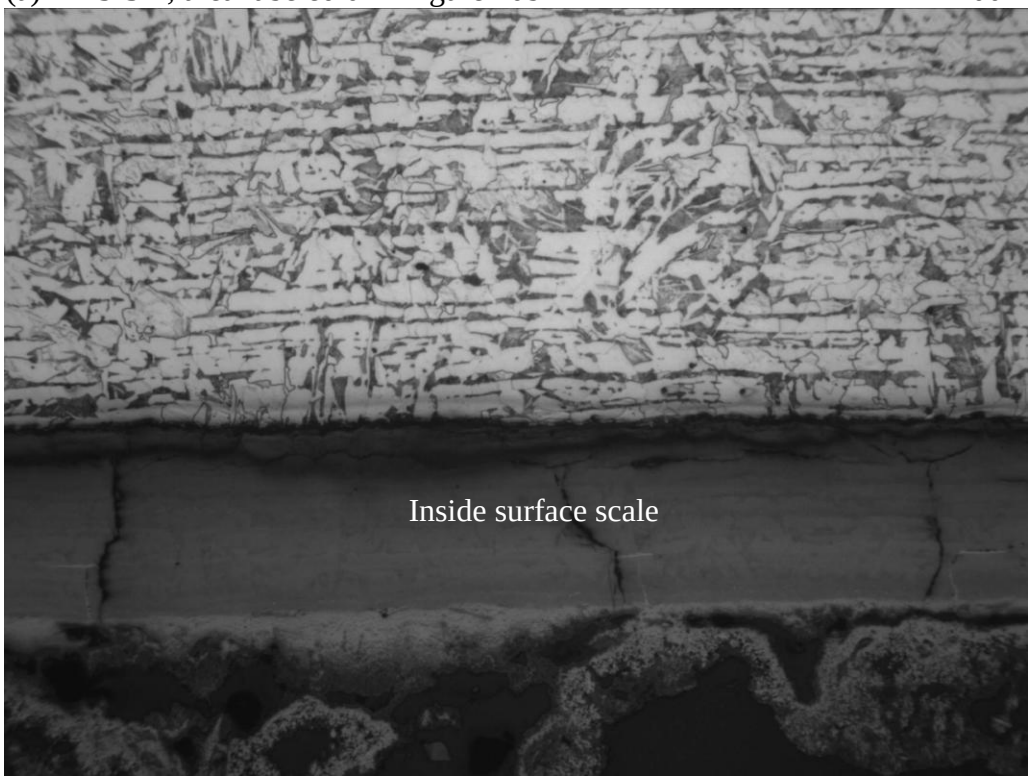

(b) ELS-5-2, area labeled χ in Figure 10b 100X

Figure 13 Optical micrographs of the specimen prepared from sample ELS-5 shown in Figure 10b. The section location is indicated in Figure 3a.

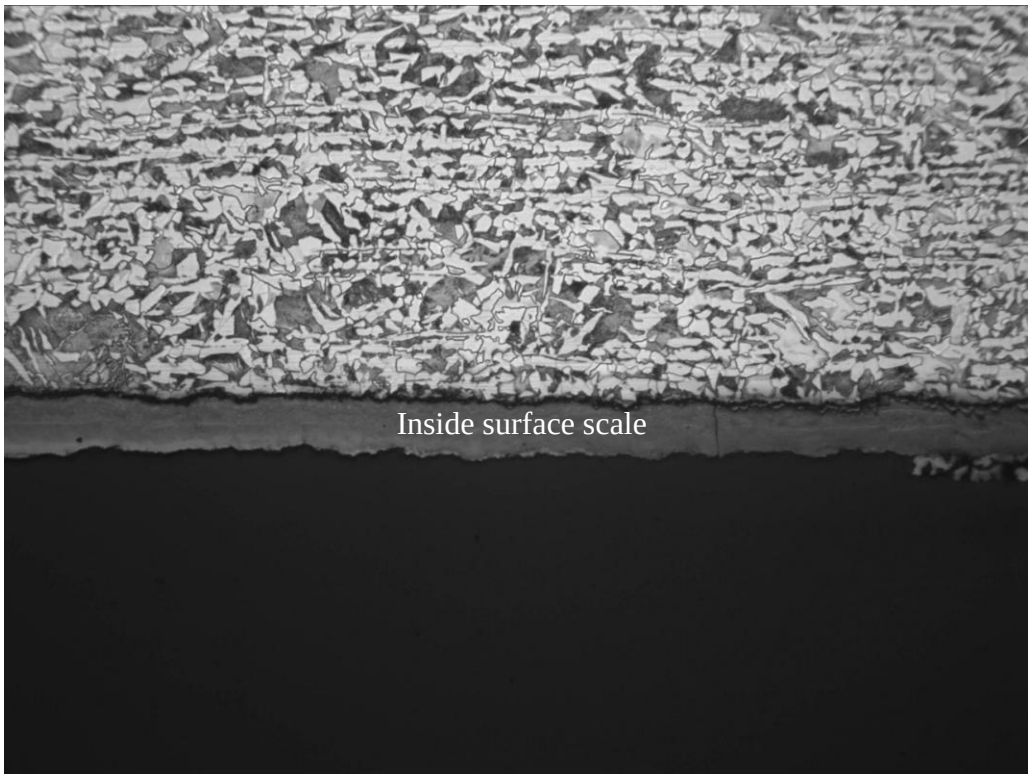

(a) ELS-6 100X

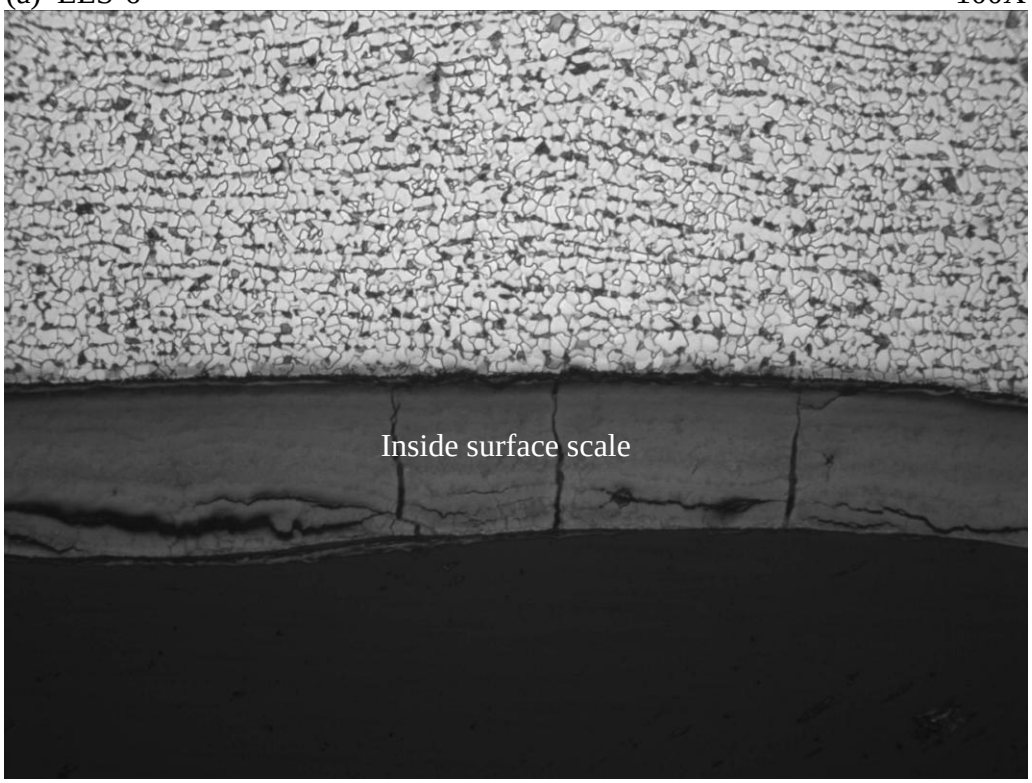

(b) ELS-7 100X

Figure 14 Optical micrographs of specimens prepared from samples ELS-6 and ELS-7. The section locations are indicated in Figure 3b and Figure 4, respectively.

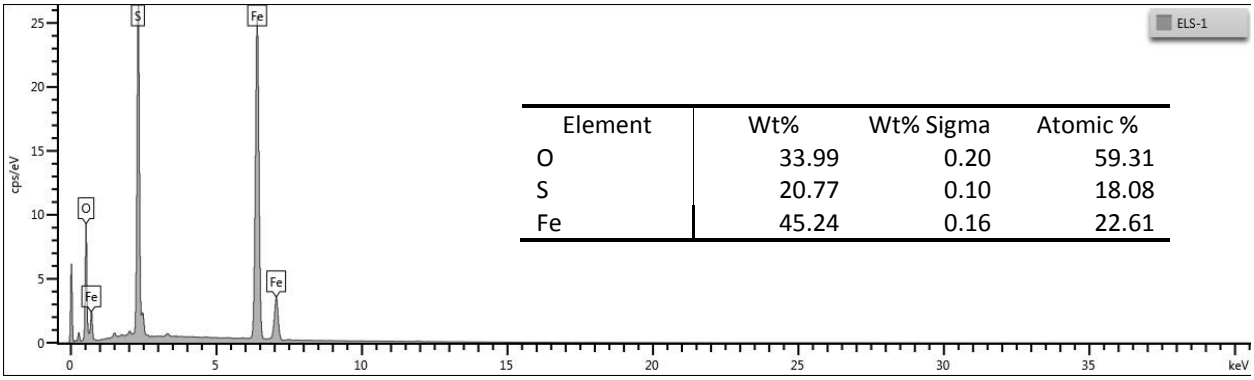

Element	Wt%	Wt% Sigma	Atomic %
O	33.99	0.20	59.31
S	20.77	0.10	18.08
Fe	45.24	0.16	22.61

(a) ELS-1

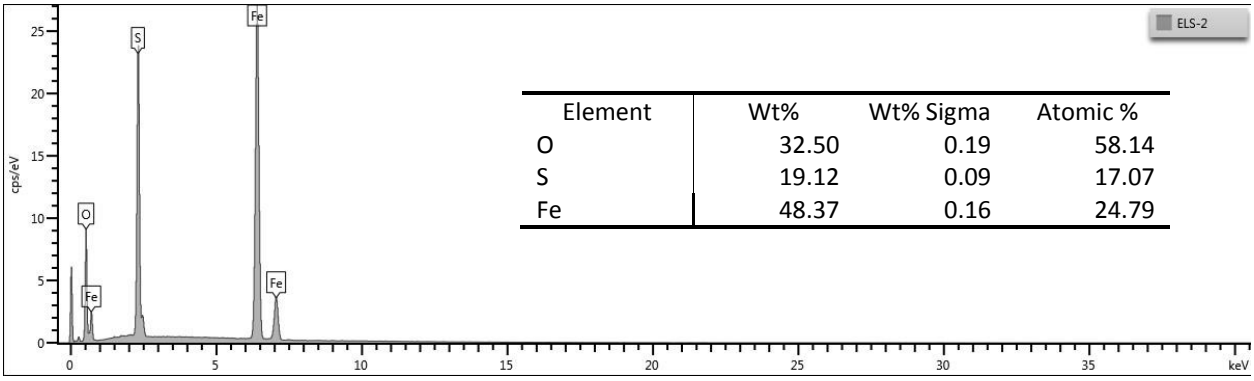

Element	Wt%	Wt% Sigma	Atomic %
O	32.50	0.19	58.14
S	19.12	0.09	17.07
Fe	48.37	0.16	24.79

(b) ELS-2

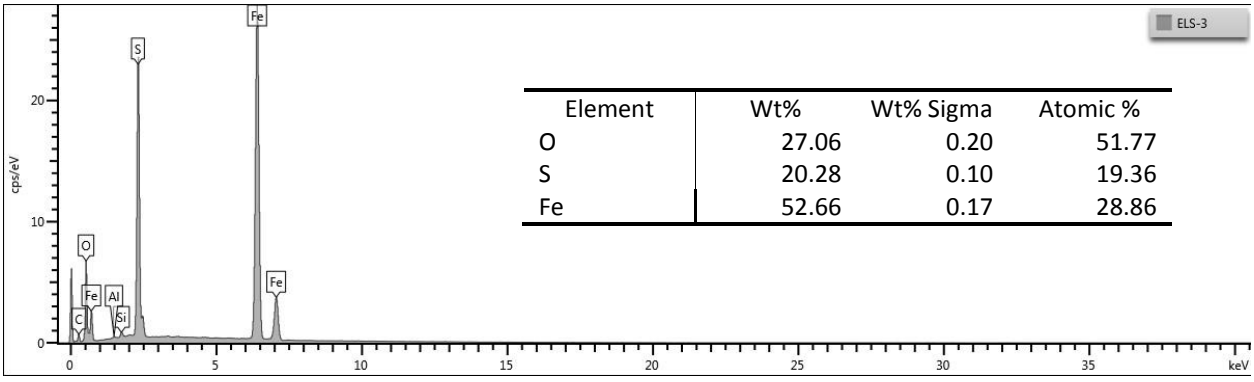

Element	Wt%	Wt% Sigma	Atomic %
O	27.06	0.20	51.77
S	20.28	0.10	19.36
Fe	52.66	0.17	28.86

(c) ELS-3

Figure 15 EDS spectra and semi-quantitative analysis results for specimens of inside surface scale scraped from samples ELS-1, ELS-2, and ELS-3.

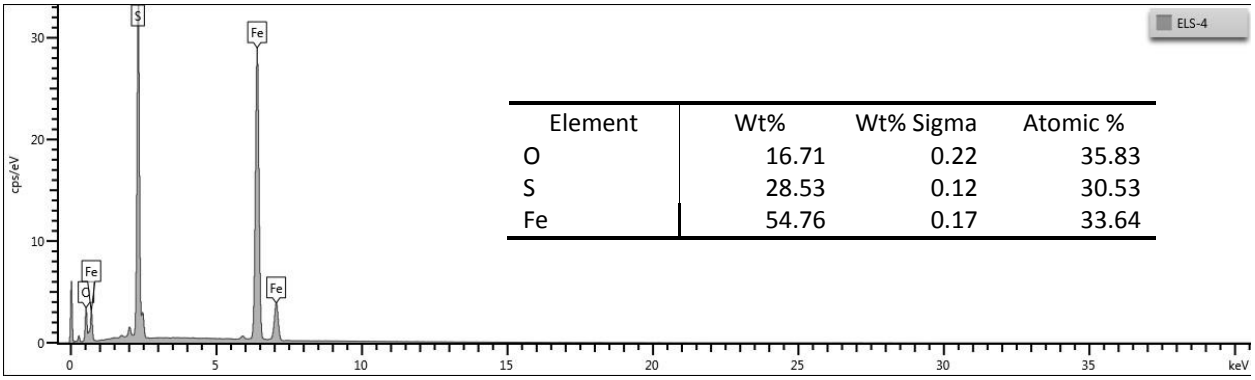

Element	Wt%	Wt% Sigma	Atomic %
O	16.71	0.22	35.83
S	28.53	0.12	30.53
Fe	54.76	0.17	33.64

ELS-4

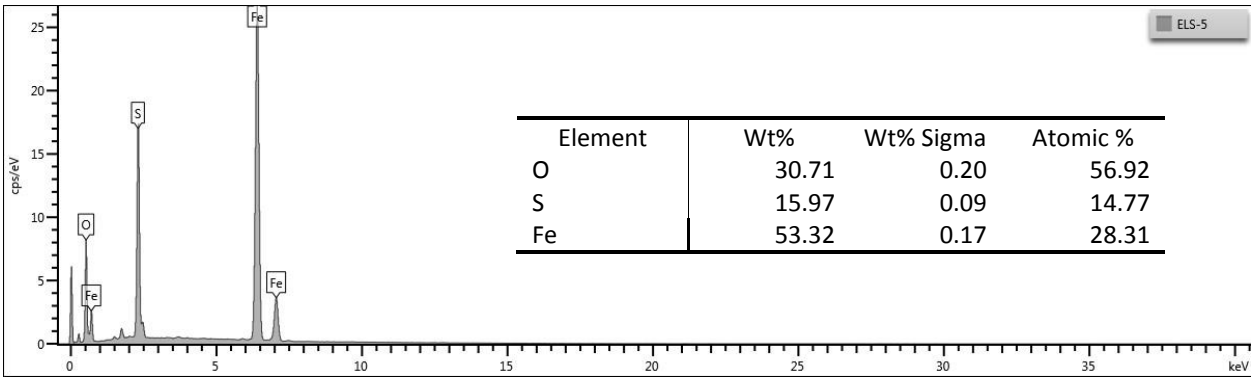

Element	Wt%	Wt% Sigma	Atomic %
O	30.71	0.20	56.92
S	15.97	0.09	14.77
Fe	53.32	0.17	28.31

ELS-5

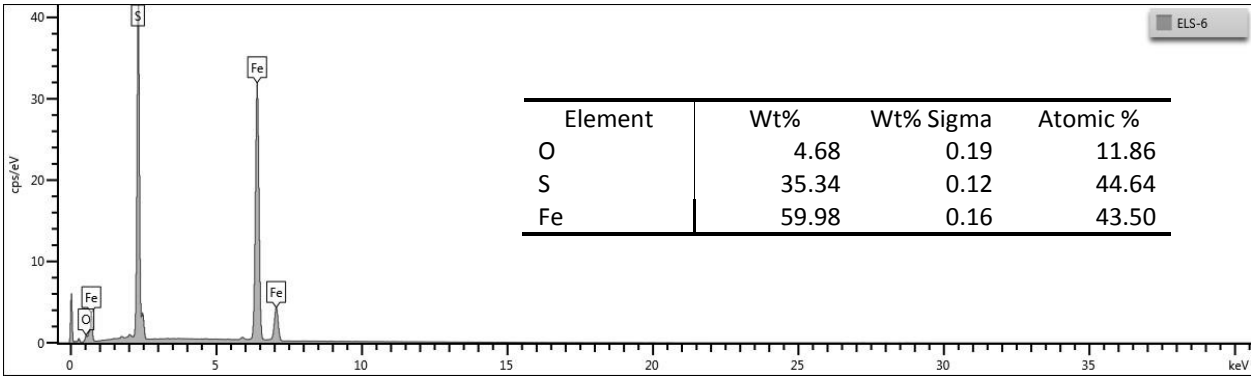

Element	Wt%	Wt% Sigma	Atomic %
O	4.68	0.19	11.86
S	35.34	0.12	44.64
Fe	59.98	0.16	43.50

ELS-6

Figure 16 EDS spectra and semi-quantitative analysis results for specimens of inside surface scale scraped from samples ELS-4, ELS-5, and ELS-6.

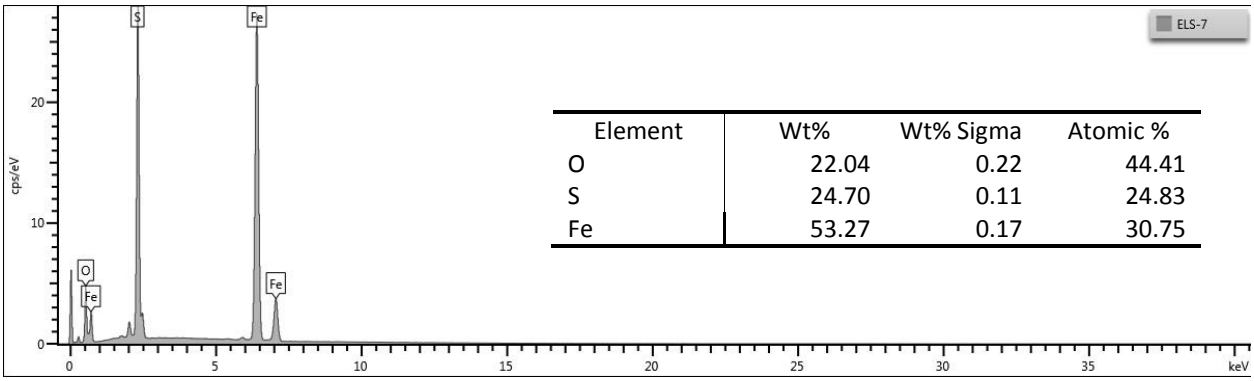

Element	Wt%	Wt% Sigma	Atomic %
O	22.04	0.22	44.41
S	24.70	0.11	24.83
Fe	53.27	0.17	30.75

ELS-7

Figure 17 EDS spectra and semi-quantitative analysis results for specimens of inside surface scale scraped from sample ELS-6.

Appendix A

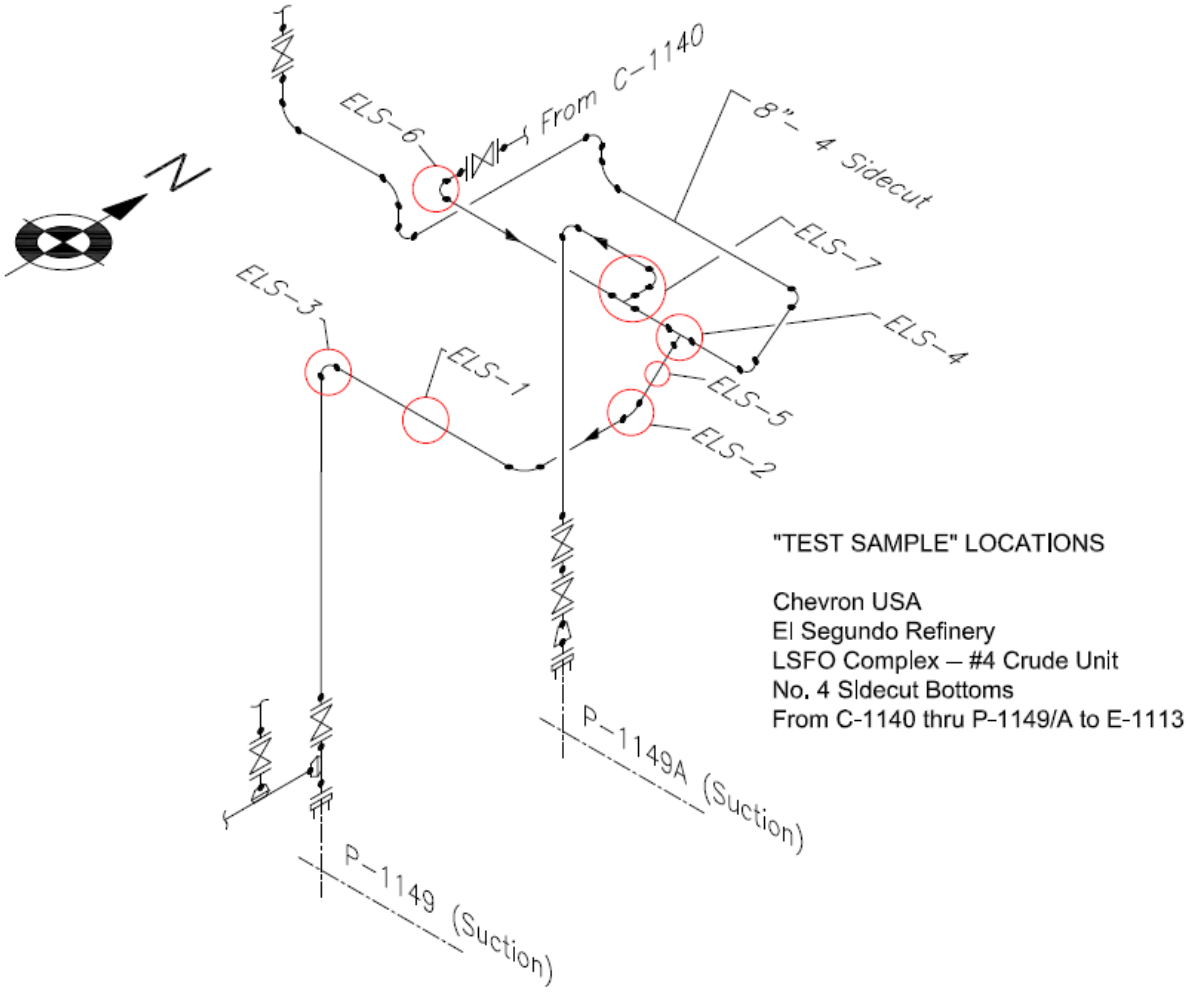
N
ELS-6
From C-1140
8"- 4 Sidecut
ELS-7
ELS-4
ELS-3
ELS-1
ELS-5
ELS-2
"TEST SAMPLE" LOCATIONS
Chevron USA
El Segundo Refinery
LSFO Complex – #4 Crude Unit
No. 4 Sidecut Bottoms
From C-1140 thru P-1149/A to E-1113
P-1149A (Suction)
P-1149 (Suction)

Appendix B

ISO 17025
Testing Cert. #2797.01

X-RAY DIFFRACTION (XRD)
ANALYSIS REPORT
07 Mar 2013

JOB NUMBER C0DHV847
PO NUMBER 15209NY

for

Norman Yuen
Anamet, Inc.
26102 Eden Landing Road, Ste. 3
Hayward, CA 94545-3811

Prepared by:

Bich Nguyen
Analyst, XRD Services
(Tel. 408-530-3834; bnguyen@eaglabs.com)

Reviewed by:

Stephen B. Robie, Ph.D.
Specialist, XRD Services
(Tel. 408-530-3638; srobie@eaglabs.com)

Evans Analytical Group
810 Kifer Rd
Sunnyvale, CA 94086 USA

Appendix B

Requester: Norman Yuen
Job Number: C0DHV847
Analysis Date: 07 Mar 2013

X-RAY DIFFRACTION ANALYSIS REPORT

Purpose: Use x-ray diffraction to identify the crystalline phases present in two scale samples. The samples were identified as ELS-4 and ELS-5.

Summary:

Best Matches from the ICDD/ICSD data bases

Sample ID	Primary Phases	Minor or Possible Trace Phases
ELS-4	$Fe_{1-x}S$ – Iron Sulfide/ Pyrrhotite -11T Hexagonal P PDF# 00-029-0726	Fe_3O_4 – Iron Oxide/Magnetite Cubic Fd-3m PDF# 00-019-0629 $FeSO_4(H_2O)_4$ – Iron Sulfate Hydrate/ Rozenite Monoclinic P21/n PDF# 01-073-1428 $Fe^{+3}O(OH)$ – Iron Oxide Hydroxide / Goethite Orthorhombic Pbnm PDF# 00-029-0713
ELS-5	$Fe_{1-x}S$ – Iron Sulfide/ Pyrrhotite -4H Hexagonal P6/mcc PDF# 00-022-1120	$Fe_{1-x}S$ – Iron Sulfide/ Pyrrhotite -4M Monoclinic A2/a PDF# 00-029-0723 Fe_3O_4 – Iron Oxide/Magnetite Cubic Fd-3m PDF# 00-019-0629 $FeSO_4(H_2O)_4$ – Iron Sulfate Hydrate/ Rozenite Monoclinic P21/n PDF# 01-073-1428 $Fe^{+3}O(OH)$ – Iron Oxide Hydroxide / Goethite Orthorhombic Pbnm PDF# 00-029-0713 FeO – Iron Oxide/Wustite Cubic Fm-3m PDF# 00-006-0615 $Ca_2(Si_9Al_3)O_{24}.8H_2O$ – Calcium Aluminum Silicate Hydrate/ Epistilbite Monoclinic C2 PDF# 00-039-1381

Appendix B

XRD Analysis Report
EAG Number C0DHV847
Norman Yuen
Anamet, Inc.

Page 3 of 7
07 Mar 2013

Results and Interpretations: The as-received samples were ground in a mortar and pestle. The resulting powders were packed into a bulk sample holder and pressed flat with a glass slide for analysis. Data was collected by a coupled Theta:2-Theta scan on a Rigaku Ultima-III in-plane diffractometer equipped with copper x-ray tube, parafocusing optics, computer-controlled fixed slits and a diffracted beam monochromator

Figure 1 compares the XRD raw data from the two samples. The position of the major pekas are similar, but there are significant differences between two samples in terms of overall intensity, peak shape and peak positions of minor peaks.

Figure 2 shows the best matches for sample ELS-4 after comparing the background-subtracted experimental data to the ICDD/ICSD diffraction database. The hexagonal Pyrrhotite-11T phase is the best match for the major phase with minor amounts of Magnetite as well. Rozenite (Iron Sulfate Hydrate) and Goethite are the best matches for trace phases in the sample.

The phase identification results for sample ELS-5 are shown in Figure 3. The peak shape near 44 degrees two-Theta indicates that this sample appears to be a mixture of the hexagonal Pyrrhotite-4H primary phase and the monoclinic Pyrrhotite-4M phase. Magnetite, Goethite minor phases as well as Rozenite and Wustite trace phases are also detected in this sample. Epistilbite (Calcium Aluminum Silicate Hydrate) appears to be present, but this match should be considered speculative because it is based only on few weak overlapping peaks.

After reviewing this report, you may assess our services using an electronic service evaluation form. This can be done by clicking on the link below, or by pasting it into your internet browser. Your comments and suggestions allow us to determine how to better serve you in the future.
http://www.eaglabs.com/main-survey.html?job=C0DHV847

Appendix B

XRD Analysis Report
EAG Number C0DHV847
Norman Yuen
Anamet, Inc.

Page 4 of 7
07 Mar 2013

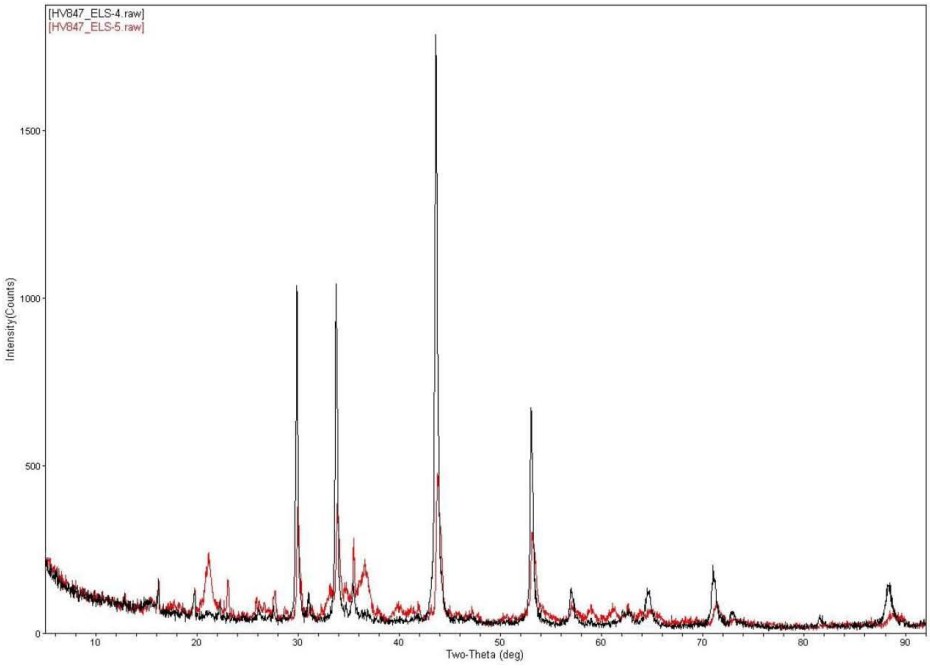

Figure 1: Comparison for two samples

Appendix B

XRD Analysis Report
EAG Number C0DHV847
Norman Yuen
Anamet, Inc.

Page 5 of 7
07 Mar 2013

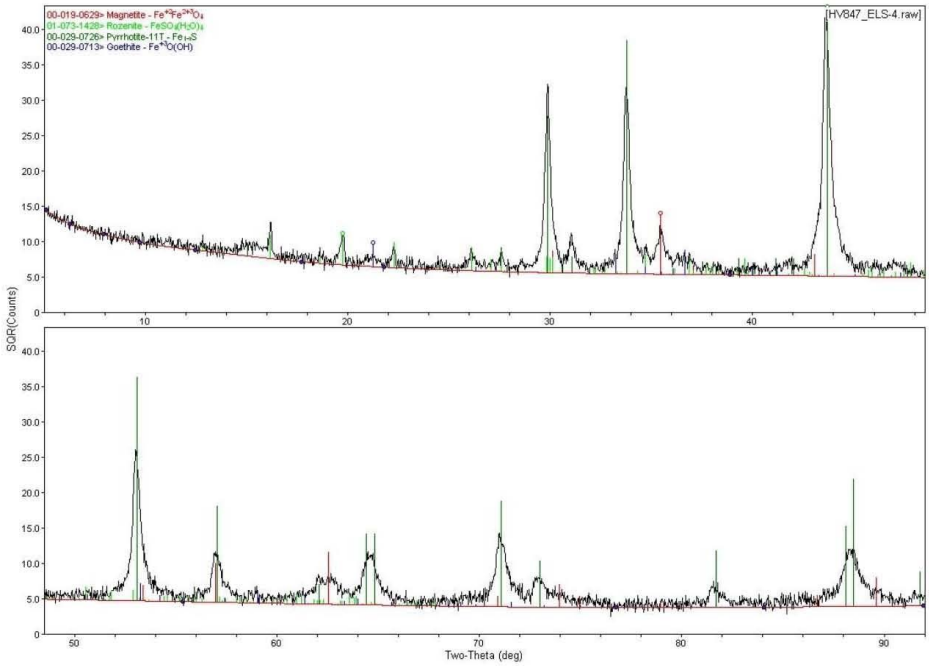

Figure 2: Phase identification for sample ELS-4

Appendix B

XRD Analysis Report
EAG Number C0DHV847
Norman Yuen
Anamet, Inc.

Page 6 of 7
07 Mar 2013

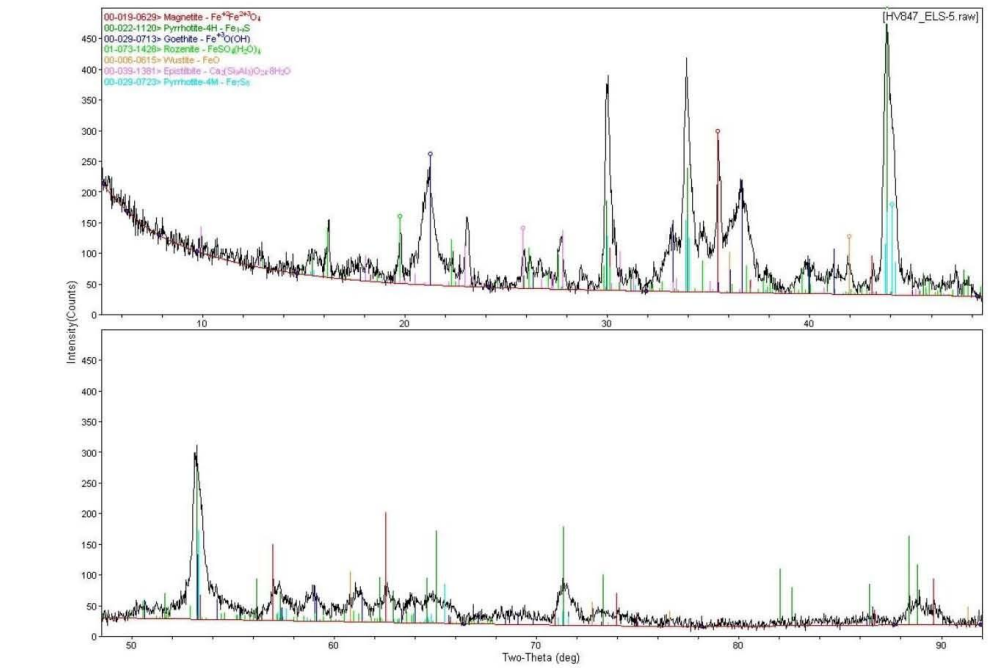

Figure 3: Phase identification for sample ELS-5

Appendix B

XRD Analysis Report
EAG Number C0DHV847
Norman Yuen
Anamet, Inc.

Page 7 of 7
07 Mar 2013

Appendix

Measurement Uncertainty:

There are two types of uncertainty in XRD analysis; uncertainty in the number of x-ray counts at a particular angle and uncertainty in the diffraction angle. Because the arrival of X-ray quanta in the detector is random with respect to time, the accuracy of X-ray counting rate measurements is governed by the laws of probability. In particular, the size of the one sigma standard deviation in an X-ray measurement is equal to the square root of the number of X-rays counted. A conservative criterion for the detection of a weak peak in a XRD pattern must have amplitude of greater than three standard deviations above background. As a result, the more slowly a measurement is made, the lower the relative standard deviation in the number of counts measured and the more likely is detection of trace diffraction peaks. If X-ray data is acquired at a constant speed, the relative standard deviation for the major diffraction peaks in a pattern will be on the order of a few percent or less while the relative standard deviation for the weaker peaks in a pattern will be on the order of tens of percent or more. This also implies that the uncertainty in the concentrations of the major phases in a sample will be lower than for the trace phases. Please note that there are a number of sample related factors that can influence peak intensity. These include (but are not limited to): average crystallite size, preferred orientation (texture), strain, and absorption.

Uncertainty in the position of X-ray diffraction peaks is due to both instrumental and sample effects. Instrumental position uncertainty is primarily due to diffractometer misalignment. Repeat measurements of NIST standard reference materials has shown that the maximum positional uncertainty is less than +/- 0.05 degrees 2-Theta and is typically much less than that. Positional uncertainty due to sample effects are related to sample displacement (displacement of the sample surface either above or below the diffractometer focusing circle) and sample transparency (the effect gets larger as the sample matrix becomes more transparent to the incident X-rays. Through careful sample preparation, the uncertainty due to these two sample effects should be less than +/- 0.03 degrees 2-Theta. Please note that in addition to these factors, solid solution effects, where one element is partially substituted for another within a given crystal structure, can produce significant shifts in measured peak positions. Unlike sample and instrumental peak position effects, solid solution effects can result in phase misidentification.